

Lessons and Open Questions from a Unified Study of Camera-Trap Species Recognition Over Time

Sooyoung Jeon^{*1} Hongjie Tian^{*1} Lemeng Wang^{*1} Zheda Mai[†] Vidhi Bakshi¹
 Jiacheng Hou¹ Ping Zhang¹ Arpita Chowdhury¹ Jianyang Gu¹ Wei-Lun Chao²

¹The Ohio State University ²Boston University

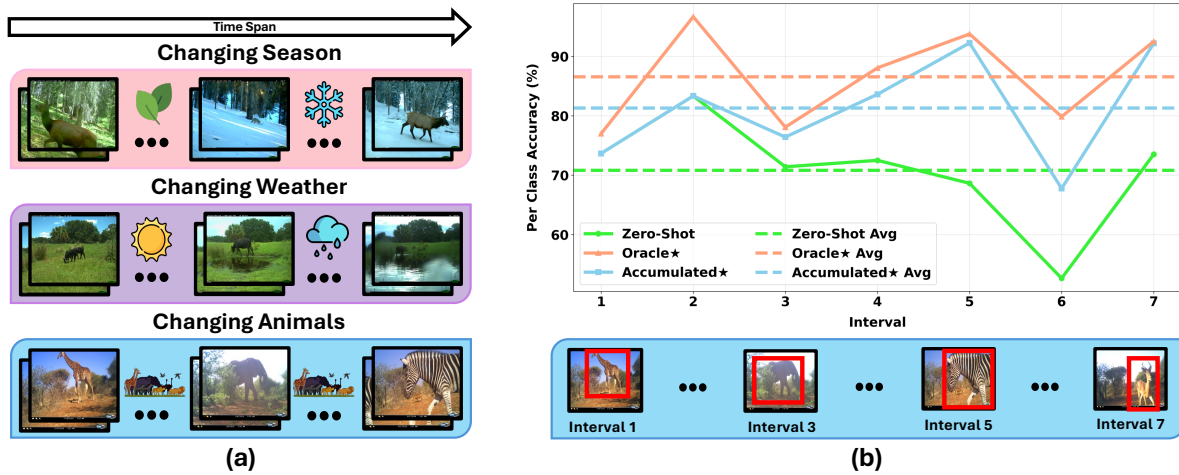


Figure 1. (a). **Temporal shifts:** even at a fixed site, foreground and background appearances evolve over time due to changing seasons, weather, and animal distribution. (b). **Streaming evaluation:** accumulated* model is fine-tuned with training data up to the current interval and evaluated on the test data of the next interval. For reference, an oracle* model is fine-tuned with the union of training data from all time intervals at a site and evaluated on the test data of all intervals. (*: our recipe Sec. 4.4).

Abstract

Camera traps are crucial for large-scale biodiversity monitoring, yet accurate automated analysis remains challenging due to diverse deployment environments. While the computer vision community has predominantly framed this challenge as cross-domain (e.g., cross-site) generalization, this perspective overlooks a primary challenge faced by ecological practitioners: maintaining reliable recognition at the fixed site over time, where the dynamic nature of ecosystems introduces profound temporal shifts in both background and animal distributions. To bridge this gap, we present the first unified study of **camera-trap species recognition over time**. We introduce a realistic, large-scale benchmark comprising 546 camera traps with a streaming protocol that evaluates models over chronologically ordered intervals. Our end-user-centric study yields four key findings. (1) Biological foundation models (e.g., Bio-

CLIP 2) underperform at numerous sites even in initial intervals, underscoring the necessity of site-specific adaptation. (2) Adaptation is challenging under realistic evaluation: when models are updated using past data and evaluated on future intervals (mirrors real deployment lifecycles), naive adaptation can even degrade below zero-shot performance. (3) We identify two main drivers of this difficulty: severe class imbalance and pronounced temporal shift in both species distribution and backgrounds between consecutive intervals. (4) We find that effective integration of model-update and post-processing techniques can largely improve accuracy, though a gap from the upper bounds remains. Finally, we highlight critical open questions, such as predicting when zero-shot models will succeed at a new site and determining whether/when model updates are necessary. Together, our benchmark and analysis provide actionable deployment guidelines for ecological practitioners while establishing new directions for future research in vision and machine learning. Training code and dataset are

^{*}Equal contribution.

[†]Corresponding author.

available at: <https://jeonso0907.github.io/stream-trap/>

1. Introduction

Camera traps are vital tools for ecology and conservation: they non-invasively capture large volumes of time-stamped images in natural habitats, supporting biodiversity monitoring, behavior analysis, and conservation planning [36, 50]. Yet ecosystems are inherently non-stationary: seasonal shifts, weather changes, vegetation growth, and animal migration constantly reshape backgrounds and animal distributions (Fig. 1a). Such dynamic conditions introduce substantial visual variability, posing unique challenges for vision models [8, 26].

Prior studies often frame the problem as domain adaptation or generalization, aiming to transfer models trained on source domains (*e.g.*, specific cameras or time periods) to unseen target domains [41, 61]. While this perspective casts camera trap data as a crucial testbed for machine learning robustness, it diverges from the practical needs of end-users (*e.g.*, ecologists and conservation practitioners). Their dominant interest is not a model’s ranking on cross-domain leaderboards, but its *ability to maintain high accuracy at a specific deployment site as dynamically changing data arrives*. Recognizing that this practical problem remains largely underexplored, we conduct a unified and comprehensive study of **camera trap species recognition over time**, reformulating the evaluation to faithfully mirror the temporal lifecycle of real-world deployments.

To facilitate this study, we introduce a realistic camera trap benchmark STREAMTRAP with a streaming evaluation protocol where models are evaluated as new data arrives and are incrementally updated thereafter. For each camera trap, the image stream is partitioned into consecutive *time intervals* for evaluating models chronologically. Concretely, at each interval j , a model can access cumulative, labeled training data from all intervals up to the j -th interval, undergo parameter updates, and evaluate on the unseen test data from the subsequent $(j + 1)$ -th interval. To construct STREAMTRAP, we curate data from the LILA BC repository [1], identifying **546** camera traps from 17 datasets, each with sufficient data spanning at least **6** months. Also, we provide a modular, reproducible data pipeline that adheres to FAIR principles (Findable, Accessible, Interoperable, and Reusable), enabling practitioners to seamlessly convert their raw ecological data into standardized temporal benchmarks.

Building on STREAMTRAP, we conduct a unified *end-user-centric* study aiming to answer common questions faced by ecological practitioners, and distill actionable guidelines for maintaining accurate models in dynamic environments. We summarize our key analyses as follows:

Adaptation is required even with biological foundation

models. End-users often face this question before deployment, especially when biological vision foundation models [19, 45] already achieve state-of-the-art zero-shot accuracy across various biodiversity datasets, including subsets of the LILA BC repository. We observe significant variability in BioCLIP 2’s **zero-shot** accuracy across 546 camera traps in STREAMTRAP: while 161 exceed 90% accuracy, demonstrating the immense promise of these models, another 162 fall in the 50–80% range, indicating a persistent, critical need for site-specific adaptation.

Adaptation is challenging in the real world. When off-the-shelf foundation models underperform, fine-tuning is a natural first adaptation choice. However, adaptation becomes more challenging than standard in-domain fine-tuning in the realistic streaming evaluation of STREAMTRAP where a model updated on data up to the current interval is evaluated on the *future* interval. Surprisingly, we find that naively supervised fine-tuning of a model (we term the **accumulated model**) using all data observed so far can degrade performance, often causing it to fall below the baseline zero-shot accuracy.

Our investigation identifies two primary drivers behind this adaptation failure. First, because camera traps acquire images passively and must “wait” for animals to appear, some species may not be observed within an interval. Thus, the training data available for an interval is often extremely low-shot and severely imbalanced, causing poor generalization during naive adaptation [49]. Second, due to the inherent non-stationarity of ecosystems, both the background context and the animal population distributions undergo profound shifts between consecutive intervals. As a result, a model that achieves high accuracy on current and past intervals is not guaranteed to maintain that performance when faced with the shifted distributions of future intervals.

Practical recipes for robust adaptation. To combat the low-shot and imbalance issues, we evaluate a suite of practical techniques and find that combining parameter-efficient fine-tuning [31] and class-imbalance losses [38, 56] is a robust solution to improve generalization in camera trap vision model adaptation. However, even with this optimized recipe, the continually adapted models still exhibit a non-negligible performance gap (Fig. 1b) compared to an upper bound (**oracle*** model fine-tuned with *all* training data across all time intervals at a site). To address the inter-interval distribution shifts and close this gap, we identify three post-processing techniques: post-hoc logit calibration [30], weight interpolation [54], and interval model selection.

More practical considerations. Accurate real-world deployment involves more than choosing an adaptation algorithm. Through discussions with end-users, we identify critical, practical questions frequently overlooked by the vision community: *How can practitioners predict if a foundation*

model’s zero-shot performance will be sufficient at a new, unseen site? If not, must we update at every interval to remain accurate, or is there an effective mechanism to determine when adapting at a given interval is actually necessary? As these questions are largely underexplored, we provide preliminary analyses and baseline solutions.

Contributions. We present the first unified study of camera trap species recognition over time that reflects the temporal lifecycle of ecological monitoring. We systematically analyze critical deployment questions, providing actionable guidance on what works while urging the computer vision community to tackle the remaining open challenges. Our work serves two primary audiences:

- **End-users:** (1) our analyses provide actionable guidance for leveraging foundation models and adaptation techniques for reliable camera-trap analysis; (2) our FAIR-compliant data preparation pipeline enables practitioners to seamlessly convert their raw ecological data into standardized benchmarks.
- **Algorithm developers:** (1) we transform the LILA BC repository (historically challenging for developers to access) into a standardized benchmark designed for evaluating robust adaptive models in the real world; (2) we identify critical, overlooked challenges about *what*, *how*, and *when* to update models under field constraints (e.g., scarce or imbalanced data, non-stationary streams). By steering development toward these practitioner-driven questions, we aim to accelerate progress in this vital scientific application area.

2. Related Work

Camera trap data in computer vision. Camera traps have become essential tools for biodiversity monitoring, capturing vast volumes of wildlife images that provide insights into species richness and behavior [10, 48]. To automate analysis, deep learning methods have been widely adopted for species detection and classification [34, 59]. A major challenge is generalization: models trained on one location often perform poorly when deployed elsewhere. The iWildCam challenges [7, 8] address this by splitting data by camera location to assess out-of-distribution generalization [26, 30]. More recently, multimodal foundation models have been applied to camera trap data for richer contextual understanding [15, 17]. However, the temporal dynamics—e.g., seasonal shifts and animal migration—remain underexplored [49]. Our benchmark incorporates temporal variability to better reflect real-world deployments.

Continual learning (CL). CL studies how a model learns from a non-stationary data stream while retaining acquired knowledge and improving over time without catastrophic forgetting. This paradigm is closely related to our streaming evaluation protocol. However, traditional CL often assumes limited or no access to past data due to privacy or

other constraints. In contrast, ecological deployments treat labeled camera trap data as a precious, persistent resource that is archived and fully accessible. To isolate temporal shift effects and avoid conflating them with artificial storage constraints, our baseline approach adopts what is typically considered an upper bound in CL: joint training on all historically available data at each interval. That said, while STREAMTRAP is explicitly tailored for studying wildlife monitoring under temporal shifts, its chronologically ordered data streams and severe, natural distribution shifts inherently provide a challenging real-world testbed for the broader continual learning community [29].

Class imbalanced learning. Camera trap datasets often follow a long-tailed distribution, where models perform well on the majority species but poorly on rare ones [9, 32]. As rare species are often of greatest ecological interest, addressing this imbalance is critical. Solutions fall into data-level and algorithm-level methods [40, 60]. We focus on simple but effective methods, such as the BSM loss [38] in our study. We provide detailed related work in Sec. A.

3. STREAMTRAP: Benchmarking Real-World Camera Trap Deployment with Streaming Evaluation Protocol

Motivation. Camera traps are central to ecology and conservation: they non-invasively capture massive streams of time-stamped images in natural habitats, enabling biodiversity monitoring, behavior analysis, and conservation planning [36, 50]. Yet the environments are inherently non-stationary: seasons, weather, vegetation, and migration continually reshape both the backgrounds and species distributions (Fig. 1a), creating persistent visual shifts for deployed vision models. Prior work typically frames this challenge as domain adaptation/generalization, focusing on transferring models from source to target domains [41, 61]. However, this framing mismatches what end-users really need. End-users do not prioritize static cross-domain leaderboards; instead, their dominant interest is a model’s *ability to maintain high accuracy at a specific deployment site over time as dynamically changing data arrives*.

Yet a benchmark that truly mirrors how camera-trap data arrives in the wild and captures the temporal lifecycle of deployments remains missing. To close this gap and refocus the community on deployment-critical evaluation, we introduce STREAMTRAP, a benchmark for camera trap species recognition over time with a streaming evaluation. By shifting the research focus from static domain transfer to site-level reliability, STREAMTRAP encourages the community to develop adaptive systems that deliver durable value in the field.

Streaming evaluation protocol. Unlike conventional domain adaptation, where data from the target domain is avail-

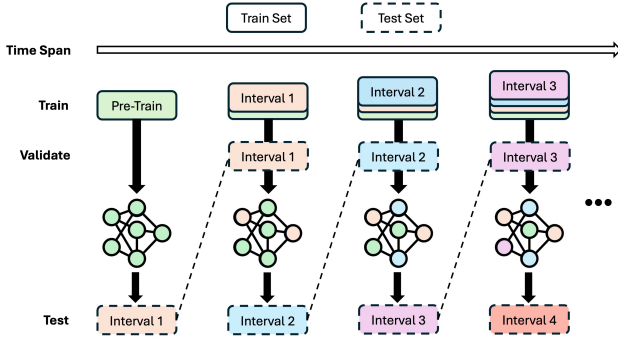


Figure 2. Streaming evaluation protocol.

able all at once [18, 44], STREAMTRAP adopts a realistic streaming evaluation that better reflects real camera-trap deployment: models are evaluated as new data arrives and are incrementally updated thereafter. Given time-stamped images from a camera trap, $\{(x_i, y_i, t_i)\}$, where x_i denotes the i -th image, y_i its label, and t_i its timestamp, we partition the stream into a sequence of chronological intervals. At interval j , a model may access the cumulative labeled training data from all intervals up to the j -th interval, update its parameters, and is then evaluated on unseen test data from the subsequent $(j+1)$ -th interval. See Fig. 2 for an illustration.

Also, while STREAMTRAP is tailored for camera traps under temporal shift, its streaming formulation also serves as an excellent, highly challenging testbed for broader machine learning paradigms, such as online continual learning [29].

3.1. Benchmark Construction and Statistics

Data source. We build STREAMTRAP on the LILA BC repository [1] with 17 camera-trap datasets (e.g., Snapshot Serengeti) comprising hundreds of camera traps deployed across continents. Here, a camera trap refers to a stationary camera installed at a fixed location to passively monitor wildlife activity.

FAIR processing pipeline. We focus on camera traps with sufficient temporal coverage and image volume to support streaming evaluation. We first partition each camera-trap stream into 30-day intervals; if an interval contains fewer than 200 images, we merge it with adjacent intervals to ensure adequate data for both training and evaluation. Within each interval, we split data into training and test subsets, constructing the test split to be **class-balanced**. Categories with fewer than 10 samples in an interval are held out as rare species to maintain evaluation stability: they are separately evaluated and analyzed in the Sec. C. To remain focused on the temporal shift problem, we follow the LILA BC protocol and apply MegaDetector [4] to extract image patches around detected animal instances. We enlarge each bounding box by 50% to preserve background context.

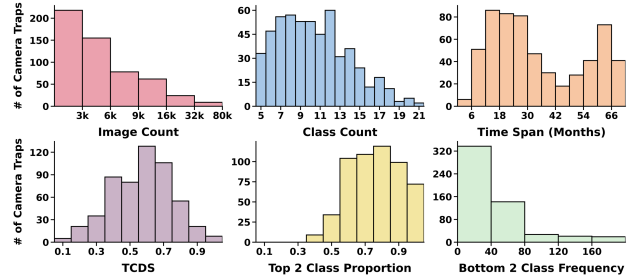


Figure 3. STREAMTRAP statistics. Top row: histograms of the image, class, and time span; Bottom row: histograms of temporal shift (TCDS, defined in Sec. 4.3) and class imbalance metrics (defined in Sec. 3.1).

To promote the FAIR principles (Findable, Accessible, Interoperable, and Reusable) and empower future researchers to convert their raw ecological data into standardized benchmarks, we establish a modular data processing pipeline. Concretely, we preprocess each camera trap to ensure the availability of essential metadata (timestamps, image-level species labels, and animal bounding boxes) and apply two main filtering steps:

1. **Single-species filtering:** retain images containing a single species (and no humans or vehicles) so that image-level labels can be unambiguously assigned to detected instances (removes $< 2\%$ of images);
2. **Detection filtering:** retain images with at least one detected animal bounding box with confidence > 0.8 to ensure correctness of the bounding box.

After filtering, we retain camera traps with more than 1,000 images and span a range of at least 6 months. Additional details, including design choices, preprocessing and pipeline steps, MegaDetector robustness checks, and the list of camera traps included, are provided in Sec. D.

Basic statistics Our rigorous processing pipeline yielded 546 valid camera traps. A summary of statistics (e.g., image and species histogram) is provided in Fig. 3. To quantify class imbalance for a camera-trap, we report two complementary metrics: (i) the fraction of images belonging to the two most frequent classes, and (ii) the number of images in the least frequent classes.

4. A Unified End-User-Centric Study

Building on STREAMTRAP, we conduct the first unified *end-user-centric* study to answer common questions faced by practitioners during deployment, and distill actionable guidelines for maintaining accurate models in dynamic environments.

Setting and model. For each camera trap, the model is initialized with the recently released BioCLIP 2 [19], a biological vision foundation model trained on biological data and capable of classifying over 800K species. To isolate the temporal dynamics we try to investigate, we assume

	C1	C2	C3	C4	C5	C6	C7	C8	C9	C10	C11	C12	C13	C14	C15	C16	C17	C18	C19	C20	Avg.
ZS	94.1	97.7	81.3	94.5	75.8	81.5	85.6	80.1	81.2	62.7	79.3	75.3	69.5	87.2	82.6	76.5	92.3	77.9	80.2	82.1	81.9
Accum	63.2	73.6	56.0	72.9	57.0	50.0	75.7	60.0	73.0	60.6	76.0	66.0	66.0	75.1	68.0	68.0	77.1	73.0	74.0	72.0	67.9
Δ	30.9	24.1	25.3	21.6	18.8	31.5	9.9	20.1	8.2	2.1	3.3	9.3	3.5	12.1	14.6	8.5	15.2	4.9	6.2	10.1	–
Accum*	98.0	98.7	79.6	94.7	76.9	69.7	94.5	75.9	88.3	75.4	90.7	80.0	79.6	88.2	81.0	80.9	89.9	84.9	85.4	83.0	84.8
Δ	3.9	1.0	1.7	0.2	1.1	11.8	8.9	4.2	7.1	14.7	11.4	4.7	10.1	1.0	1.6	4.4	2.4	7.0	5.2	0.9	–
Oracle*	96.1	98.7	84.9	96.5	84.3	82.2	90.0	81.6	91.0	89.7	92.1	82.4	78.7	90.3	87.8	87.0	96.4	91.6	87.8	86.8	88.8
Δ	2.0	1.0	3.6	2.0	8.5	0.7	4.4	1.5	9.8	27.0	12.8	7.1	9.2	3.1	5.2	10.5	4.1	13.7	7.6	4.7	–

Table 1. Accuracy difference (Δ) between accumulated (Accum) and oracle models against zero-shot (ZS). Blue (red) denotes improvement (degradation) relative to ZS. *: our adaptation recipe (Sec. 4.4)

the candidate set of species expected at each camera trap is known a priori. This assumption closely aligns with real-world deployments, where practitioners typically possess prior knowledge of the local fauna derived from historical observations or metadata. To ensure the broader generalizability of our findings, we provide additional experiments in the Sec. C for scenarios where species are unknown beforehand.

Evaluation metric. For each camera trap, we compute a model’s average per-class accuracy within each interval (Balanced Accuracy), and then average these values across all intervals to obtain the overall performance.

4.1. Is Adaptation still Required with Foundation Models?

In practice, ecological practitioners often face this pressing question before deployment, especially as recent biological vision foundation models [19, 45] already achieve state-of-the-art zero-shot accuracy across various biodiversity datasets, including subsets of the LILA BC repository.

Zero-shot baseline. We begin by evaluating the zero-shot performance of BioCLIP 2 for all 546 camera traps in STREAMTRAP. To construct the zero-shot classifier head, we utilize each species’ common name as the text label and apply OpenAI’s standard prompt templates to generate the text embeddings. Formally, let f_θ denote the pre-trained vision encoder and w_c the L2-normalized text embedding of class c . Given an image patch x , the predicted class is $\hat{y} = \arg \max_c w_c^\top f_\theta(x)$. As illustrated in Fig. 4a, we observe a significant variability in zero-shot accuracy across 546 camera traps: BioCLIP 2 exceeds 90% accuracy on 161 camera traps, highlighting its strong potential in wildlife monitoring, yet 162 camera traps fall in the 50–80% range. This wide performance spread suggests that while zero-shot models provide a strong baseline, **there remains a persistent, critical need for site-specific adaptation.** We include zero-shot results for other foundation models in the Sec. B for reference.

4.2. Adaptation is Challenging in the Real World.

When end-users find that off-the-shelf foundation models underperform at their camera traps, the natural next step is to *adapt* them using labeled data collected at that site over time. The streaming evaluation protocol in STREAMTRAP is designed to mirror this real-world deployment lifecycle (Sec. 3). Concretely, for a given camera trap at interval j , the model is updated with the cumulative labeled training data collected up to the j -th interval, and is subsequently evaluated on the test data from the $(j + 1)$ -th interval.

Preliminary study. Supervised fine-tuning is arguably the most common adaptation strategy. We introduce the **accumulated model** as the baseline, which naively fine-tunes on *all* training data collected up to interval j . We initialize the base model with BioCLIP 2, consistent with the zero-shot model described above. The model is fine-tuned using a standard cross-entropy loss and a cosine learning rate scheduler with a base learning rate of 2.5×10^{-5} . We re-emphasize that under our evaluation, test data is exclusively drawn from the future interval $(j+1)$. To ensure the generalizability of our findings, we select 20 representative camera traps for this preliminary study, strategically sampled to span a wide spectrum of zero-shot accuracies. Surprisingly, as shown in Tab. 1, naive accumulated fine-tuning *consistently underperforms* the zero-shot baseline with a large margin. Notably, this baseline is already optimistic: it uses all historical labeled data at each update step and does not impose any computation or storage constraints. The fact that this unconstrained, accumulated fine-tuning still underperforms the zero-shot baseline starkly underscores the **severe generalization challenges inherent to realistic camera trap temporal adaptation**, which motivates a *deeper diagnosis of the underlying drivers of failure*. More experimental details and comprehensive results are provided in the Sec. C.



Figure 4. (a). Zero-shot performance across camera traps. **Blue**: above 90% accuracy; **red**: below 80%. (b). Accuracy difference between oracle naive fine-tuning and zero-shot. **Blue**: oracle outperforms zero-shot; **red**: zero-shot is superior. (c). Accuracy difference between oracle fine-tuning with our adaptation recipe (Oracle*) and zero-shot.

4.3. Diagnosing the Drivers of Adaptation Challenges

We hypothesize that the severe adaptation difficulties may stem from two distinct but compounding factors: (1) the inter-interval distribution shifts driven by temporal non-stationarity; (2) the inherent difficulty of the camera trap.

Intrinsic difficulty even without temporal shift. To disentangle these factors, we first consider a deliberately *cheating* setting that removes the effect of inter-interval shift. Specifically, we train an **oracle** model using *all* labeled training data across *all* time intervals at a site, and evaluate it on held-out test data (thus matching the standard i.i.d.-style training paradigm more closely). Under this simplified setting, one might expect the oracle to consistently outperform the zero-shot baseline. Surprisingly, this is not the case: on 214/546 camera traps ($\sim 40\%$), the oracle model still underperforms the zero-shot model (Fig. 4b). This result indicates that temporal shift is not the sole source of difficulty; rather, the *optimization and generalization challenges inherent to camera-trap data* are already substantial even when train and test distributions are more aligned.

Diving deeper into the data characteristics, we observe that because camera traps acquire images passively (waiting for animals to appear), many species are rarely observed within a given timeframe. This fundamental mechanism inherently produces extreme class imbalance within each camera trap. As shown in Fig. 3, the top two majority classes typically dominate, accounting for an average of $\sim 71\%$ of the total images per camera trap. Compounding this issue, the minority classes exist in an extremely low-shot regime: on average, the two least-frequent classes contain only ~ 49 images in a camera trap, compared to ~ 4500 images for the two majority classes. Attempting to fine-tune a foundation model on such severely imbalanced, low-shot data inevitably introduces bias, amplifies memorization, and ultimately harms generalization.

Temporal shift is pervasive. The inherent non-stationarity of natural ecosystems causes both the background context

(vegetation, illumination, weather) and the animal population distributions to undergo profound shifts between consecutive intervals, as illustrated in Fig. 5. To formally quantify the *animal class distribution shift* between consecutive intervals, we propose the Temporal Class Distribution Shift (TCDS) metric for a specific camera trap. For class c at interval j , let the normalized class frequency be $p_j^c = \frac{n_j^c}{\sum_k n_j^k}$, where n_j^c is the sample count of class c in interval j . We can define:

$$\text{TCDS} := \underbrace{\frac{1}{n-1} \sum_{j=1}^{n-1}}_{\text{Average over all intervals}} \underbrace{\sum_c |p_j^c - p_{j+1}^c|}_{\text{Class distribution shift between intervals}}$$

TCDS captures the average magnitude of temporal shift in class distributions across all consecutive intervals for a camera trap. As illustrated in Fig. 5 (Bottom), this metric effectively quantifies class distribution shifts across example camera traps, where higher TCDS values correspond to greater temporal shifts. Unfortunately, a substantial fraction of the camera traps exhibit exceptionally high TCDS values (Fig. 3). Thus, a model that achieves high accuracy on the current interval is fundamentally not guaranteed to maintain that performance when confronted with the drastically shifted data distributions of future intervals.

Compounding effects. These two primary drivers (severe data imbalance and profound temporal shifts) become entangled in practice. They create a compounding effect that renders continual adaptation exceptionally difficult during real-world streaming evaluations. This diagnosis motivates the need for an effective, robust recipe that enables end-users to maintain reliably accurate models in dynamic environments.

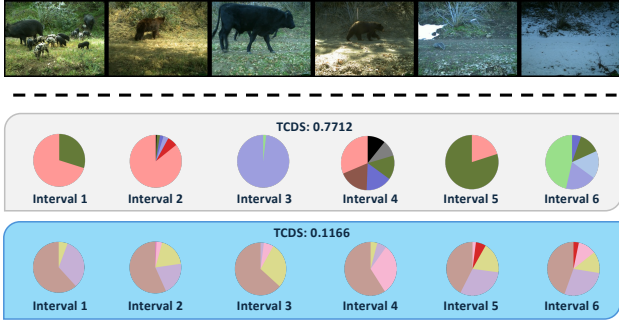


Figure 5. **Illustration of temporal shifts.** (Top) A camera trap showing shifting context over time. (Bottom) Pie charts (class frequency per interval) comparing two camera traps: the first camera exhibits higher temporal shifts ($\text{TCDS}=0.7712$) than the second ($\text{TCDS}=0.1166$).

4.4. Practical Recipes for Robust Adaptation.

In this section, we explore machine learning techniques that can overcome the adaptation challenges discussed above, ultimately establishing a practical and effective “first-to-try” adaptation recipe for end-users.

Improving Generalization. We first focus on strategies to mitigate the severe generalization degradation caused by extreme class imbalance and low-shot data. Motivated by prior literature on long-tailed recognition and efficient adaptation [31, 60], we investigate two primary directions:

Class-imbalanced loss. Standard cross-entropy fine-tuning on severely imbalanced data inherently biases the model toward majority classes, yielding poor generalization across classes [13, 56, 57]. Class-imbalanced loss functions offer a simple and effective mitigation. We explore several established methods, including Balanced Softmax (BSM) [39], Class-Balanced Focal Loss (CB-Focal) [12], and Class-Dependent Temperatures (CDT) [58]. As detailed in our ablation studies (Sec. B), we find that BSM delivers consistent improvements across camera traps without requiring hyperparameter tuning, whereas CB-Focal and CDT require more hyperparameter tuning, which is often infeasible for camera trap deployments. We therefore adopt BSM as our default imbalance-aware loss: $\mathcal{L}_{\text{BSM}}(\mathbf{x}, y) = -\log\left(\frac{n_y \exp(\eta_y(\mathbf{x}))}{\sum_c n_c \exp(\eta_c(\mathbf{x}))}\right)$ where $\eta_c(\mathbf{x}) = \mathbf{w}_c^\top f_\theta(\mathbf{x})$ denotes the logit for class c , and n_c is the number of training instances for class c .

Parameter-Efficient Fine-Tuning (PEFT). Fully fine-tuning on imperfect data often risks corrupting the generalized representations inherent to foundation models [31]. Unlike full fine-tuning, which updates all network parameters, PEFT modifies only a minimal subset of weights, thereby preserving pre-trained knowledge [31]. We evaluate three representative PEFT approaches: Low-Rank Adaptation (LoRA) [22], Visual Prompt Tuning (VPT) [25],

and Adapter Tuning [21]. Our ablations (Sec. B) demonstrate that LoRA, which introduces trainable low-rank matrices into the attention projection layers, achieves superior performance without heavy hyperparameter tuning. Consequently, we adopt LoRA as our default fine-tuning mechanism.

Synergy between imbalance loss and PEFT. To rigorously assess the isolated and combined impacts of these two directions, we conduct an ablation study on a representative subset of 20 camera traps with the oracle setting. We observe that applying either the imbalance loss (BSM) or PEFT (LoRA) in isolation yields only marginal improvements (less than 1%) over naive full fine-tuning. However, combining BSM + LoRA yields a substantial, compounding performance boost, strongly suggesting their compatibility and complementarity. Motivated by this result, we consider the **BSM + LoRA** as our recommended adaptation recipe for camera traps (denoted hereafter as \star). Applying this recipe to the oracle models (oracle \star) across all 546 camera traps in the STREAMTRAP benchmark enables 474 sites (compared to only 332 for the naive oracle) to successfully outperform the zero-shot baseline (Fig. 4c). While there remain 72 camera traps where this recipe falls short, we provide a detailed qualitative and quantitative analysis of these specific failure cases in Sec. C.

Mitigating Temporal Shifts. Our proposed adaptation recipe (\star) successfully transfers its effectiveness from the idealized oracle setting to the accumulated model evaluated under the realistic streaming protocol. As shown in Tab. 1, the accumulated model equipped with our recipe (denoted as accum \star) consistently outperforms the zero-shot baseline. However, a non-negligible performance gap persists between the accum \star models and corresponding upper bounds (the oracle \star models) on certain camera traps. This discrepancy is primarily driven by inter-interval distribution shifts, which inherently complicate streaming evaluations. Mitigating such temporal shifts is notoriously difficult due to the unpredictability of future data distributions, a challenge that remains largely underexplored in the vision community. To bridge this gap, we evaluate various approaches and identify three promising post-processing techniques that can potentially improve the accum \star model.

Post-hoc logit calibration. When some classes are absent or extremely low-shot during fine-tuning, the updated model tends to heavily suppress their predicted logits relative to the majority classes, even if the foundation model originally represented them well [30, 49]. To rectify this bias, we adopt a post-hoc logit calibration [30] to boost the logits of absent or minority classes to a magnitude comparable to the majority classes by introducing a calibration factor γ [30]: $\hat{y} = \arg \max_c \mathbf{w}_c^\top f_\theta(\mathbf{x}) + \gamma \cdot \mathbf{1}[c \in \mathcal{A}]$, where \mathcal{A} denotes absent/minority classes in the current interval.

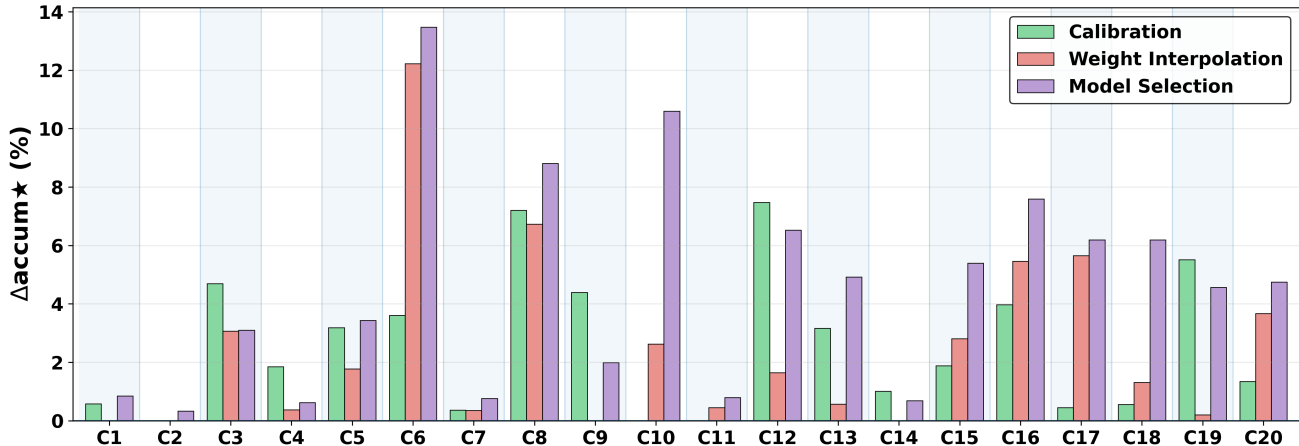


Figure 6. Performance gain (Δaccum^\star) of calibration, weight interpolation, and model selection over the accum^\star baseline. They are applied on top of accum^\star . More results in Sec. C.

Weight interpolation. While fine-tuning enables necessary task-specific adaptation, it risks forgetting of the foundation model’s broad generalization capabilities. To strike a balance between generalizable pre-trained knowledge and site-specific features, we apply weight interpolation (WiSE) [54]. Let θ' be the fine-tuned weights and θ the pre-trained weights. The interpolated weights are given by $\theta(\alpha) = \alpha\theta + (1 - \alpha)\theta'$ where $\alpha \in [0, 1]$ controls the interpolation ratio.

Interval model selection. Because we cannot observe future data at update time, the most recently adapted model is not necessarily the best match for the next interval: due to recurring seasonal patterns or abrupt changes, interval $(j+1)$ may resemble an earlier interval more than the most recent one. To investigate the feasibility of exploiting this phenomenon, we conduct a preliminary study in which we explicitly select the historical and current model that attains the highest accuracy on the test split of interval $j + 1$.

Promises and limits of post-processing. Fig. 6 illustrates the relative gains each post-processing method offers over the baseline accum^\star model. Notably, for the subset of camera traps that initially underperformed the zero-shot baseline, at least one of these post-processing methods can recover the performance drop. Moreover, these techniques can effectively narrow the gap between the oracle^\star and accum^\star models, underscoring their tremendous potential for mitigating temporal shift. However, we emphasize that we evaluate these approaches in an optimistic, upper-bound setting: selecting the performance-maximizing hyperparameters to illustrate the potential of these methods. In real deployments, selecting hyperparameters without access to future data remains a key open problem. We view this as an important research opportunity and encourage future work on principled mechanisms to resolve the degradation caused by temporal shifts

Recommended Adaptation Recipes

We recommend combining **LoRA** (PEFT) with **BSM** (imbalance loss) as a practical first-to-try adaptation strategy, augmented by post-processing techniques, such as **logit calibration**, **weight interpolation**, or **interval model selection**, to compact inter-interval distribution shift.

5. More practical considerations

Accurate real-world deployment involves more than selecting an adaptation algorithm. Practically, key questions include when a foundation model is sufficient, whether continual adaptation is necessary, and when adaptation should occur. Despite their importance for real-world deployment, they remain largely underexplored in the vision community. This section provides preliminary analyses with simple baselines and highlights several directions for future research.

5.0.1. When is the zero-shot model sufficient?

In real-world deployments, practitioners must predict whether a foundation model’s zero-shot performance is sufficient for a new site. If yes, the model can be deployed directly without data collection and adaptation. However, this decision must typically be made before labeled data from the new site are available, making zero-shot accuracy hard to estimate in advance. Despite its practical importance, this problem remains largely underexplored in the vision community. As a simple baseline, we assess if out-of-distribution (OOD) signals can provide an indication of zero-shot accuracy [55]. The intuition is that if images from a new camera trap are closer to the training distribution, the model may produce higher-confidence predictions and achieve better zero-shot accuracy. Specifically,

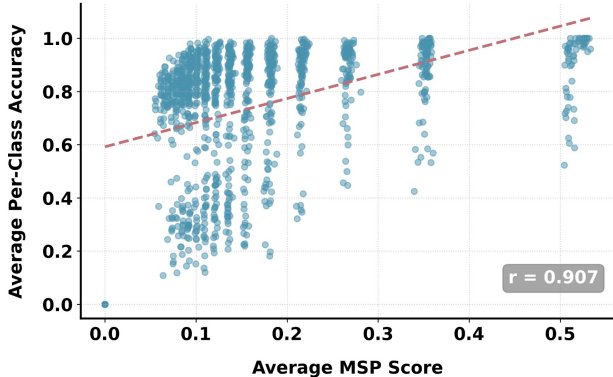


Figure 7. Non-OOD scores (MSP) correlate with zero-shot.

we adopt the Maximum Softmax Probability (MSP) [20], assigning each test sample a non-OOD score: $s_{\text{MSP}}(\mathbf{x}) = \max_c \frac{\exp(\eta_c(\mathbf{x})/\tau)}{\sum_{c'} \exp(\eta_{c'}(\mathbf{x})/\tau)}$ where $\eta_c(\mathbf{x}) = \mathbf{w}_c^\top f_\theta(\mathbf{x})$ denotes the logit for class c , and τ is a temperature parameter. We plot the average non-OOD score for each camera trap against the zero-shot accuracy in Fig. 7. While a positive correlation can be observed, many camera traps deviate from this pattern, indicating that confidence signals alone are insufficient to reliably predict zero-shot performance. This highlights the difficulty of estimating zero-shot sufficiency prior to deployment, suggesting it as an open problem for future work.

Stage	0%	25%	50%	75%	100%
Acc.	76.2	73.1	77.8	82.7	84.9

Table 2. Accum* frozen at a specific interval (e.g., 25% = adapted on first 25% of intervals) and evaluated on all future intervals. Averaged across 8 camera traps (12+ intervals each).

5.0.2. Do we need continual adaptation?

Another practical question raised by end-users is: once a model has been updated over several initial intervals and has sufficiently learned site-specific characteristics, will it generalize well enough to handle all future data without further fine-tuning? To empirically investigate this, we conduct a controlled study where adaptation is deliberately halted after a fixed number of intervals. Specifically, for camera traps with long deployment durations (spanning more than one year), the accumulated model is frozen at a specific interval and subsequently evaluated on all remaining future intervals. As demonstrated in Tab. 2, model accuracy generally improves as it is adapted on progressively more intervals. This trend clearly indicates that continually assimilating additional site-specific data over time yields compounding performance benefits. But our analysis also reveals that not all temporal updates are strictly necessary. Because certain intervals provide significantly richer adap-

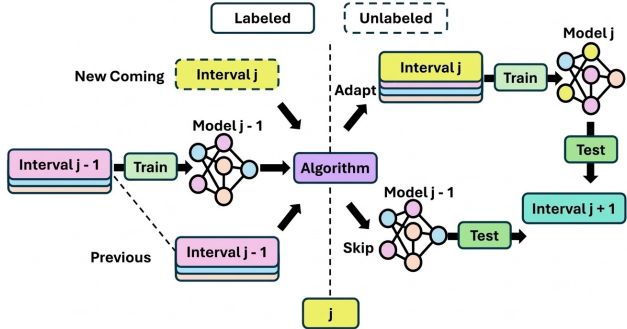


Figure 8. The Adapt-or-Skip problem described below.

tation signals than others, the marginal performance gain of updating fluctuates. This crucial observation motivates our next investigation: can we algorithmically determine *when* an adaptation step is actually required?

5.0.3. When Should We Adapt?

Adaptation incurs labeling and computational costs, making it crucial to determine when it is truly beneficial. However, this decision must be made before observing future performance, making it challenging in practice. At every interval, the end-users will face an **Adapt-or-Skip** problem: should we adapt at this interval or not? Despite its practical importance, this remains largely underexplored. Formally, at interval j , the end-user only has access to the previously trained model j_{-1} , prior labeled intervals ($1 \dots j - 1$), and current unlabeled interval j . As illustrated in Fig. 8, the end-user must decide, before observing the test data of interval $j+1$, whether to **adapt** the model using interval j (train model j) or **skip** adaptation and continue using model j_{-1} . The correct decision is defined as whichever choice yields higher accuracy on the interval $j+1$ test data. We construct a dataset where half of the intervals favor adapting and half favor skipping. We evaluate three simple baseline methods: random, MSP-based, and CLIP feature-based. However, both methods perform similarly to random guessing, highlighting the difficulty of the problem. For reference, we report an upper-bound that always selects the correct decision, which outperforms the three baselines by 11.34%, suggesting substantial room for future research. More details are provided in Appendix.

6. Conclusion

We present the first study of camera-trap species recognition over time, prioritizing reliable, long-term fixed-site deployment. Our benchmark, STREAMTRAP, uses a streaming evaluation protocol reflecting real-world data collection. Because naive foundation model fine-tuning fails under extreme data imbalance and temporal shifts, we provide robust adaptation recipes and analyze critical deployment challenges to guide practitioners and spur future research.

Acknowledgment

This research is supported by grants from the National Science Foundation (ICICLE: OAC-2112606). We are grateful for the support of the Ohio Supercomputer Center for providing computational resources.

References

- [1] Lila bc: Labeled information library of alexandria: Biology and conservation. <https://lila.science/>. 2, 4
- [2] Rahaf Aljundi, Min Lin, Baptiste Goujaud, and Yoshua Bengio. Gradient based sample selection for online continual learning. *Advances in neural information processing systems*, 32, 2019. 1
- [3] Victor Anton, Stephen Hartley, Andre Geldenhuis, and Heiko U Wittmer. Monitoring the mammalian fauna of urban areas using remote cameras and citizen science. *Journal of Urban Ecology*, 4(1):juy002, 2018. 8
- [4] Sara Beery. The MegaDetector: Large-scale deployment of computer vision for conservation and biodiversity monitoring. In *AI for Social Impact*. Cambridge University Press, 2023. 4, 6
- [5] Sara Beery, Grant Van Horn, and Pietro Perona. Recognition in terra incognita. In *Proceedings of the European conference on computer vision (ECCV)*, pages 456–473, 2018. 6, 8
- [6] Sara Beery, Grant Van Horn, and Pietro Perona. Recognition in terra incognita. In *Proceedings of the European conference on computer vision (ECCV)*, pages 456–473, 2018. 1
- [7] Sara Beery, Grant Van Horn, Oisín Mac Aodha, and Pietro Perona. The iwildcam 2018 challenge dataset. *arXiv preprint arXiv:1904.05986*, 2019. 3, 1
- [8] Sara Beery, Arushi Agarwal, Elijah Cole, and Vighnesh Birodkar. The iwildcam 2021 competition dataset. *arXiv preprint arXiv:2105.03494*, 2021. 2, 3, 1
- [9] Peggy A Bevan, Omiros Pantazis, Holly Pringle, Guilherme Braga Ferreira, Daniel J Ingram, Emily Madsen, Liam Thomas, Dol Raj Thanet, Thakur Silwal, Santosh Rayamajhi, et al. Deep learning-based ecological analysis of camera trap images is impacted by training data quality and quantity. *arXiv preprint arXiv:2408.14348*, 2024. 3, 2
- [10] Luigi Boitani. *Camera trapping for wildlife research*. Pelagic Publishing Ltd, 2016. 3, 1
- [11] Ludwig Bothmann, Lisa Wimmer, Omid Charrakh, Tobias Weber, Hendrik Edelhoff, Wibke Peters, Hien Nguyen, Caryl Benjamin, and Annette Menzel. Automated wildlife image classification: An active learning tool for ecological applications. *Ecological Informatics*, 77:102231, 2023. 1
- [12] Yin Cui, Menglin Jia, Tsung-Yi Lin, Yang Song, and Serge Belongie. Class-balanced loss based on effective number of samples, 2019. 7, 2
- [13] Yin Cui, Menglin Jia, Tsung-Yi Lin, Yang Song, and Serge Belongie. Class-balanced loss based on effective number of samples. In *Proceedings of the IEEE/CVF conference on computer vision and pattern recognition*, pages 9268–9277, 2019. 7
- [14] Matthias De Lange, Rahaf Aljundi, Marc Masana, Sarah Parisot, Xu Jia, Aleš Leonardis, Gregory Slabaugh, and Tinne Tuytelaars. A continual learning survey: Defying forgetting in classification tasks. *IEEE transactions on pattern analysis and machine intelligence*, 44(7):3366–3385, 2021. 1
- [15] Zalan Fabian, Zhongqi Miao, Chunyuan Li, Yuanhan Zhang, Ziwei Liu, Andrés Hernández, Andrés Montes-Rojas, Rafael Escucha, Laura Siabatto, Andrés Link, et al. Multimodal foundation models for zero-shot animal species recognition in camera trap images. *arXiv preprint arXiv:2311.01064*, 2023. 3, 1
- [16] Abolfazl Farahani, Sahar Voghoei, Khaled Rasheed, and Hamid R Arabnia. A brief review of domain adaptation. *Advances in data science and information engineering: proceedings from ICDATA 2020 and IKE 2020*, pages 877–894, 2021. 1
- [17] Valentin Gabeff, Marc Rußwurm, Devis Tuia, and Alexander Mathis. Wildclip: Scene and animal attribute retrieval from camera trap data with domain-adapted vision-language models. *International Journal of Computer Vision*, 132(9): 3770–3786, 2024. 3, 1
- [18] Boqing Gong, Yuan Shi, Fei Sha, and Kristen Grauman. Geodesic flow kernel for unsupervised domain adaptation. In *2012 IEEE conference on computer vision and pattern recognition*, pages 2066–2073. IEEE, 2012. 4
- [19] Jianyang Gu, Samuel Stevens, Elizabeth G Campolongo, Matthew J Thompson, Net Zhang, Jiaman Wu, Andrei Kopanav, Zheda Mai, Alexander E White, James Balhoff, et al. Bioclip 2: Emergent properties from scaling hierarchical contrastive learning. *arXiv preprint arXiv:2505.23883*, 2025. 2, 4, 5
- [20] Dan Hendrycks and Kevin Gimpel. A baseline for detecting misclassified and out-of-distribution examples in neural networks. *arXiv preprint arXiv:1610.02136*, 2016. 9
- [21] Neil Houlsby, Andrei Giurgiu, Stanislaw Jastrzebski, Bruna Morrone, Quentin de Laroussilhe, Andrea Gesmundo, Mona Attariyan, and Sylvain Gelly. Parameter-efficient transfer learning for nlp, 2019. 7, 2
- [22] Edward J Hu, Yelong Shen, Phillip Wallis, Zeyuan Allen-Zhu, Yuanzhi Li, Shean Wang, Lu Wang, Weizhu Chen, et al. Lora: Low-rank adaptation of large language models. *ICLR*, 1(2):3, 2022. 7, 2
- [23] Idaho Department of Fish and Game. Idaho camera traps. <https://lila.science/datasets/idaho-camera-traps/>. 8
- [24] IUCN SSC Asian Wild Cattle Specialist Group’s Saola Working Group. Northern and central annamites camera traps 2.0. Dataset, 2021. SWG (2021). 6
- [25] Menglin Jia, Luming Tang, Bor-Chun Chen, Claire Cardie, Serge Belongie, Bharath Hariharan, and Ser-Nam Lim. Visual prompt tuning, 2022. 7, 2
- [26] Pang Wei Koh, Shiori Sagawa, Henrik Marklund, Sang Michael Xie, Marvin Zhang, Akshay Balsubramani, Weihua Hu, Michihiro Yasunaga, Richard Lanus Phillips, Irena Gao, et al. Wilds: A benchmark of in-the-wild distribution shifts. In *International conference on machine learning*, pages 5637–5664. PMLR, 2021. 2, 3, 1

- [27] Tsung-Yi Lin, Michael Maire, Serge Belongie, James Hays, Pietro Perona, Deva Ramanan, Piotr Dollár, and C Lawrence Zitnick. Microsoft coco: Common objects in context. In *European conference on computer vision*, pages 740–755. Springer, 2014. 6
- [28] Zheda Mai, Ruiwen Li, Hyunwoo Kim, and Scott Sanner. Supervised contrastive replay: Revisiting the nearest class mean classifier in online class-incremental continual learning. In *Proceedings of the IEEE/CVF conference on computer vision and pattern recognition*, pages 3589–3599, 2021. 1
- [29] Zheda Mai, Ruiwen Li, Jihwan Jeong, David Quispe, Hyunwoo Kim, and Scott Sanner. Online continual learning in image classification: An empirical survey. *Neurocomputing*, 469:28–51, 2022. 3, 4, 1
- [30] Zheda Mai, Arpita Chowdhury, Ping Zhang, Cheng-Hao Tu, Hong-You Chen, Vardaan Pahuja, Tanya Berger-Wolf, Song Gao, Charles Stewart, Yu Su, et al. Fine-tuning is fine, if calibrated. *Advances in Neural Information Processing Systems*, 37:136084–136119, 2024. 2, 3, 7, 1
- [31] Zheda Mai, Ping Zhang, Cheng-Hao Tu, Hong-You Chen, Quang-Huy Nguyen, Li Zhang, and Wei-Lun Chao. Lessons and insights from a unifying study of parameter-efficient fine-tuning (peft) in visual recognition. In *Proceedings of the Computer Vision and Pattern Recognition Conference*, pages 14845–14857, 2025. 2, 7
- [32] Farjad Malik, Simon Wouters, Ruben Cartuyvels, Erfan Ghadery, and Marie-Francine Moens. Two-phase training mitigates class imbalance for camera trap image classification with cnns. *arXiv preprint arXiv:2112.14491*, 2021. 3, 2
- [33] New Zealand Trailcams. Trail camera images of new zealand animals. <https://lila.science/datasets/nz-trailcams>. 8
- [34] Mohammad Sadegh Norouzzadeh, Anh Nguyen, Margaret Kosmala, Alexandra Swanson, Meredith S Palmer, Craig Packer, and Jeff Clune. Automatically identifying, counting, and describing wild animals in camera-trap images with deep learning. *Proceedings of the National Academy of Sciences*, 115(25):E5716–E5725, 2018. 3, 1
- [35] Lain E Pardo, Sara Bombaci, Sarah E Huebner, Michael J Somers, Herve Fritz, Colleen Downs, Abby Guthmann, Robyn S Hetem, Mark Keith, Aliza le Roux, et al. Snapshot safari: A large-scale collaborative to monitor africa’s remarkable biodiversity. *South African Journal of Science*, 117(1-2):1–4, 2021. 8
- [36] Laura J Pollock, Justin Kitzes, Sara Beery, Kaitlyn M Gaynor, Marta A Jarzyna, Oisín Mac Aodha, Bernd Meyer, David Rolnick, Graham W Taylor, Devis Tuia, et al. Harnessing artificial intelligence to fill global shortfalls in biodiversity knowledge. *Nature Reviews Biodiversity*, pages 1–17, 2025. 2, 3
- [37] Alec Radford, Jong Wook Kim, Chris Hallacy, Aditya Ramesh, Gabriel Goh, Sandhini Agarwal, Girish Sastry, Amanda Askell, Pamela Mishkin, Jack Clark, Gretchen Krueger, and Ilya Sutskever. Learning transferable visual models from natural language supervision, 2021. 2
- [38] Jiawei Ren, Cunjun Yu, Xiao Ma, Haiyu Zhao, Shuai Yi, et al. Balanced meta-softmax for long-tailed visual recognition. *Advances in neural information processing systems*, 33:4175–4186, 2020. 2, 3
- [39] Jiawei Ren, Cunjun Yu, Shunan Sheng, Xiao Ma, Haiyu Zhao, Shuai Yi, and Hongsheng Li. Balanced meta-softmax for long-tailed visual recognition, 2020. 7, 2
- [40] Salim Rezvani and Xizhao Wang. A broad review on class imbalance learning techniques. *Applied Soft Computing*, 143:110415, 2023. 3, 2
- [41] Shiori Sagawa, Pang Wei Koh, Tony Lee, Irena Gao, Sang Michael Xie, Kendrick Shen, Ananya Kumar, Weihua Hu, Michihiro Yasunaga, Henrik Marklund, et al. Extending the wilds benchmark for unsupervised adaptation. *arXiv preprint arXiv:2112.05090*, 2021. 2, 3
- [42] Julian D Santamaria, Claudia Isaza, and Jhony H Giraldo. Catalog: A camera trap language-guided contrastive learning model. In *2025 IEEE/CVF Winter Conference on Applications of Computer Vision (WACV)*, pages 1197–1206. IEEE, 2025. 1
- [43] Dongsu Shim, Zheda Mai, Jihwan Jeong, Scott Sanner, Hyunwoo Kim, and Jongseong Jang. Online class-incremental continual learning with adversarial shapley value. In *Proceedings of the AAAI Conference on Artificial Intelligence*, pages 9630–9638, 2021. 1
- [44] Peeyush Singhal, Rahee Walambe, Sheela Ramanna, and Ketan Kotecha. Domain adaptation: challenges, methods, datasets, and applications. *IEEE access*, 11:6973–7020, 2023. 4
- [45] Samuel Stevens, Jiaman Wu, Matthew J Thompson, Elizabeth G Campolongo, Chan Hee Song, David Edward Carlyn, Li Dong, Wasila M Dahdul, Charles Stewart, Tanya Berger-Wolf, et al. Bioclip: A vision foundation model for the tree of life. In *Proceedings of the IEEE/CVF conference on computer vision and pattern recognition*, pages 19412–19424, 2024. 2, 5
- [46] Alexandra Swanson, Margaret Kosmala, Chris Lintott, Robert Simpson, Arfon Smith, and Craig Packer. Snapshot serengeti, high-frequency annotated camera trap images of 40 mammalian species in an african savanna. *Scientific data*, 2(1):1–14, 2015. 1, 6, 8
- [47] Michael A Tabak, Mohammad S Norouzzadeh, David W Wolfson, Steven J Sweeney, Kurt C VerCauteren, Nathan P Snow, Joseph M Halseth, Paul A Di Salvo, Jesse S Lewis, Michael D White, et al. Machine learning to classify animal species in camera trap images: Applications in ecology. *Methods in Ecology and Evolution*, 10(4):585–590, 2019. 6, 8
- [48] Franck Trollet, Cédric Vermeulen, Marie-Claude Huynen, and Alain Hambuckers. Use of camera traps for wildlife studies: a review. *Biotechnologie, Agronomie, Société et Environnement*, 18(3), 2014. 3, 1
- [49] Cheng-Hao Tu, Hong-You Chen, Zheda Mai, Jike Zhong, Vardaan Pahuja, Tanya Berger-Wolf, Song Gao, Charles Stewart, Yu Su, and Wei-Lun Harry Chao. Holistic transfer: towards non-disruptive fine-tuning with partial target data. *Advances in Neural Information Processing Systems*, 36:29149–29173, 2023. 2, 3, 7

- [50] Devis Tuia, Benjamin Kellenberger, Sara Beery, Blair R Costelloe, Silvia Zuffi, Benjamin Risse, Alexander Mathis, Mackenzie W Mathis, Frank Van Langevelde, Tilo Burghardt, et al. Perspectives in machine learning for wildlife conservation. *Nature communications*, 13(1):792, 2022. [2](#), [3](#)
- [51] Grant Van Horn, Oisín Mac Aodha, Yang Song, Yin Cui, Chen Sun, Alex Shepard, Hartwig Adam, Pietro Perona, and Serge Belongie. The inaturalist species classification and detection dataset. In *Proceedings of the IEEE conference on computer vision and pattern recognition*, pages 8769–8778, 2018. [6](#)
- [52] Delia Velasco-Montero, Jorge Fernández-Berni, Ricardo Carmona-Galán, Ariadna Sanglas, and Francisco Palomares. Reliable and efficient integration of ai into camera traps for smart wildlife monitoring based on continual learning. *Ecological Informatics*, 83:102815, 2024. [1](#)
- [53] Juliana Vélez, William McShea, Hila Shamon, Paula J Castiblanco-Camacho, Michael A Tabak, Carl Chalmers, Paul Fergus, and John Fieberg. An evaluation of platforms for processing camera-trap data using artificial intelligence. *Methods in Ecology and Evolution*, 14(2):459–477, 2023. [8](#)
- [54] Mitchell Wortsman, Gabriel Ilharco, Jong Wook Kim, Mike Li, Simon Kornblith, Rebecca Roelofs, Raphael Gontijo Lopes, Hannaneh Hajishirzi, Ali Farhadi, Hongseok Namkoong, et al. Robust fine-tuning of zero-shot models. In *Proceedings of the IEEE/CVF conference on computer vision and pattern recognition*, pages 7959–7971, 2022. [2](#), [8](#)
- [55] Jingkang Yang, Kaiyang Zhou, Yixuan Li, and Ziwei Liu. Generalized out-of-distribution detection: A survey. *International Journal of Computer Vision*, 132(12):5635–5662, 2024. [8](#)
- [56] Han-Jia Ye, Hong-You Chen, De-Chuan Zhan, and Wei-Lun Chao. Identifying and compensating for feature deviation in imbalanced deep learning. *arXiv preprint arXiv:2001.01385*, 2020. [2](#), [7](#)
- [57] Han-Jia Ye, De-Chuan Zhan, and Wei-Lun Chao. Procrustean training for imbalanced deep learning. In *Proceedings of the IEEE/CVF international conference on computer vision*, pages 92–102, 2021. [7](#)
- [58] Han-Jia Ye, Hong-You Chen, De-Chuan Zhan, and Wei-Lun Chao. Identifying and compensating for feature deviation in imbalanced deep learning, 2022. [7](#), [2](#)
- [59] Xiaoyuan Yu, Jiangping Wang, Roland Kays, Patrick A Jansen, Tianjiang Wang, and Thomas Huang. Automated identification of animal species in camera trap images. *EURASIP Journal on Image and Video Processing*, 2013(1): 52, 2013. [3](#), [1](#)
- [60] Yifan Zhang, Bingyi Kang, Bryan Hooi, Shuicheng Yan, and Jiashi Feng. Deep long-tailed learning: A survey. *IEEE transactions on pattern analysis and machine intelligence*, 45(9):10795–10816, 2023. [3](#), [7](#), [2](#)
- [61] Kaiyang Zhou, Ziwei Liu, Yu Qiao, Tao Xiang, and Chen Change Loy. Domain generalization: A survey. *IEEE transactions on pattern analysis and machine intelligence*, 45(4):4396–4415, 2022. [2](#), [3](#)
- [62] Haowei Zhu, Ye Tian, and Junguo Zhang. Class incremental learning for wildlife biodiversity monitoring in camera trap images. *Ecological Informatics*, 71:101760, 2022. [1](#)

Lessons and Open Questions from a Unified Study of Camera-Trap Species Recognition Over Time

Supplementary Material

In this supplementary material, we provide more details and experiment results in addition to the main paper:

- Sec. A: Detailed Related Work
- Sec. B: Adaptation Recipe: Details and Ablations
- Sec. C: Additional Details and Results
- Sec. D: STREAMTRAP: Construction Details

A. Detailed Related Work

A.1. Camera Trap Data in Computer Vision

Large-scale wildlife image collections captured through camera traps have emerged as invaluable resources for biodiversity monitoring, providing critical insights into species richness, occupancy patterns, and animal behaviors [10, 48]. These automated imaging systems generate substantial volumes of visual data, typically requiring extensive off-site manual analysis. To alleviate this bottleneck, deep neural networks have been increasingly adopted for automating tasks such as species detection and classification, positioning camera trap datasets as pivotal resources within the computer vision and machine learning communities [34, 59].

A significant research direction involves the generalization capabilities of models trained on camera trap data [26, 30]. Specifically, systems trained to detect and classify animals are frequently deployed in novel geographical locations without subsequent fine-tuning. To accurately reflect this practical constraint, the widely recognized iWild-Cam challenges [7, 8] deliberately partition their datasets by camera location. This ensures no overlap between training and test camera locations, providing a robust evaluation of model generalization to unseen environments. Additionally, with the advent of multimodal foundation models, camera trap imagery has increasingly been integrated into multimodal analysis frameworks to enhance wildlife monitoring through richer contextual understanding [15, 17]. In parallel, CATALOG [42] demonstrates that combining multiple foundation models within a contrastive learning framework improves zero-shot camera trap recognition across Snapshot Serengeti [46] and Terra Incognita [6]. Recent work also emphasizes label efficiency and practitioner usability: Bothmann et al. propose an active-learning-based pipeline that couples object detection, careful hyperparameter tuning, and iterative query strategies to train accurate wildlife classifiers from relatively small, region-specific camera trap datasets [11].

While existing literature largely frames camera trap analysis as a cross-domain generalization problem, this perspective diverges from the practical needs of end-users such as ecologists and conservation practitioners. Their primary concern is sustaining reliable species recognition at a **fixed deployment site over time**, where seasonal variations, habitat changes, and animal migration continuously reshape both animal appearances and backgrounds, causing model performance to degrade substantially over extended deployments. To address this critical gap, we conduct a **unified, end-user-centric study** that reframes evaluation around the actual deployment lifecycle, systematically characterizing adaptation challenges and deriving actionable guidelines for long-term camera trap deployment.

A.2. Continual Learning

Unlike conventional domain adaptation settings [14, 16], where data with distribution shifts are available all at once, continual learning deals with models that must adapt to non-stationary data streams over time [29]. A key challenge is maintaining reliable performance as distributions shift, whether from new classes, changing backgrounds, or evolving environmental conditions [2, 28, 43]. However, most existing benchmarks artificially partition datasets without actual timestamps, creating evaluation scenarios that are either unrealistically simple or excessively challenging [29].

Recently, Velasco-Montero et al. demonstrated how continual learning could be embedded into smart camera traps for efficient deployment, but their focus was primarily on hardware and system design [52]. Zhu et al. studied class-incremental learning for wildlife monitoring but did not account for the real temporal order in camera trap data [62]. More broadly, conventional continual learning assumes limited access to past data due to privacy or storage constraints, an assumption that does not hold in ecological deployments where labeled camera trap data is a persistent, archivable resource. We therefore train on the full historical record at each interval to reflect this reality, naturally exposing temporal non-stationarity as the central challenge, and providing a real-world testbed grounded in genuine ecological dynamics for the broader continual learning community.

A.3. Class Imbalanced Learning

The distribution of animal classes in camera trap datasets is often highly imbalanced. Models trained on such an imbalanced dataset are often heavily biased, performing exceptionally well on majority classes while underperforming

significantly on minority classes [9, 32]. However, models that achieve balanced performance across all classes are more valuable, especially considering that rare classes are often of particular ecological interest. Techniques designed to mitigate class imbalance in deep learning can be broadly categorized into two groups: data-level methods, which modify the data distribution directly by oversampling or undersampling, and algorithm-level methods, which adjust the learning process itself through specialized loss functions or other algorithmic modifications. For a comprehensive review of these approaches, we refer readers to recent surveys [40, 60]. In our study, we specifically explore simple yet highly effective algorithm-level methods, such as the Balanced Softmax loss [38], to address class imbalance issues in camera trap datasets.

B. Adaptation Recipe: Details and Ablations

BioCLIP 2 [19]	CLIP [37]
84.3	72.3

Table A1. Zero-shot baseline selection. Average per-class accuracy (%) across all camera traps in the STREAMTRAP. BioCLIP 2 is selected as the zero-shot baseline due to its superior performance.

B.1. Zero-shot Baseline

We adopt BioCLIP 2 [19] as our zero-shot baseline, as it delivers the strongest zero-shot performance on all camera traps in STREAMTRAP. As shown in Tab. A1, BioCLIP 2 achieves an average zero-shot per-class accuracy of 84.3%, substantially outperforming CLIP [37]. This gap reflects BioCLIP 2’s pre-training on large-scale biological imagery, which enables it to better capture the fine-grained appearance variation inherent to camera trap data.

Hyperparameter	Value
Optimizer	AdamW
Max Learning Rate	2.5×10^{-5}
Min Learning Rate	4.17×10^{-7}
Weight Decay	1×10^{-4}
LR Schedule	Cosine Annealing ($T_{\max} = 60$)
Batch Size	32

Table A2. Training configuration for fine-tuning BioCLIP 2.

B.2. Training Details

We fine-tune BioCLIP 2 using the configuration summarized in Tab. A2. We employ early stopping based on validation performance. For the oracle model, the validation set is constructed by randomly sampling two images per class from the training set. For the accumulated model at interval j , we use the test split of the preceding interval $j-1$ as the validation set.

Loss	FT Method	Accuracy
CE	Full	85.9
BSM [39]	Full	85.1
CB-Focal [12]	Full	83.2
CDT [58]	Full	83.2
CE	LoRA [22]	86.0
CE	VPT [25]	76.6
CE	Adapter [21]	85.3
BSM [39]	LoRA [22]	90.3

Table A3. Ablation of imbalance losses and PEFT fine-tuning (FT) methods. Average per-class accuracy (%) is reported. BSM and LoRA achieve the best performance. Our proposed adaptation recipe (★) is highlighted in blue.

B.3. Ablation of Imbalance Loss and PEFT

We ablate imbalance losses and PEFT methods under the oracle setting to identify the most effective combination. Since evaluating all configurations across 546 camera traps in STREAMTRAP is computationally expensive, we sub-sample 20 camera traps spanning the full range of accuracy gaps between naive oracle and zero-shot, ensuring coverage of both easy and challenging scenarios.

Imbalance loss comparison. As shown in Fig. 3, severe class imbalance is a defining characteristic of camera traps in STREAMTRAP, where a few dominant species account for most observations while many others appear only sparsely. Training with standard cross-entropy biases the classifier toward majority classes, diminishing its ability to recognize minority species (Sec. A.3). To evaluate imbalance-aware training objectives, we compare three widely used methods: Balanced Softmax (BSM) [39], Class-Balanced Focal Loss (CB-Focal; $\beta=0.999, \gamma=0.5$) [12], and Class-Dependent Temperatures (CDT; $\gamma=0.3$) [58]. Notably, BSM requires no additional hyperparameters, whereas CB-Focal and CDT require tuning.

PEFT comparison. Unlike full fine-tuning, which risks corrupting the generalized representations of the foundation model, PEFT methods update only a minimal subset of parameters to better preserve pre-trained knowledge. We compare three representative approaches: Low-Rank Adaptation (LoRA; $r=8$) [22], which introduces learnable low-rank matrices into all attention projection layers; Visual Prompt Tuning (VPT-Deep; 10 prompt tokens per layer) [25], which steers the model by augmenting the input sequence with learnable tokens; and Adapter Tuning (bottleneck dimension = 8, $\alpha=1.0$) [21], which inserts lightweight bottleneck modules after both the attention and MLP sublayers. In all cases, only the newly introduced parameters are updated while the backbone remains frozen.

From ablation to recipe. As shown in Tab. A3, BSM yields the best average performance among the three imbalance losses, while CB-Focal and CDT exhibit performance degradation. For PEFT, LoRA consistently outperforms both VPT and adapter tuning, aligning with recent studies showing its stability in low-data regimes. We further examine the compatibility of the best-performing method from each direction. Moreover, BSM and LoRA are not only compatible but complementary: their combination yields the strongest and most consistent performance, where LoRA contributes stable and efficient adaptation while BSM effectively mitigates the severe class imbalance inherent in camera-trap streams. We therefore adopt BSM and LoRA as our recommended adaptation recipe (\star).

C. Additional Details and Results

C.1. Evaluating Beyond Assumptions

In the Sec. 3 and Sec. 4, we adopt two assumptions to maintain evaluation stability and mirror real-world deployment: a closed-set species vocabulary and the exclusion of rare species within each interval. To ensure the generalizability of our findings, we relax each assumption below. For both analyses, we evaluate ten camera traps sampled randomly.

	Closed-Set	Open-Set	Closed-Set + Rare Species
Zero-shot	82.5	37.8	73.1
Accum \star	83.7	76.7	73.4
Oracle \star	88.3	86.1	66.8

Table A4. Average per-class accuracy (%) under relaxed evaluation assumptions. Open-Set expands the vocabulary to all 1,096 classes across STREAMTRAP. Rare Species adds rare classes (fewer than 10 samples per interval) to the test set.

Open-set classification. In Sec. 4, we assume the candidate species at each camera trap are known a priori (closed-set), allowing us to isolate temporal dynamics. Here, we relax this assumption by constructing an open-set vocabulary from all 1,096 classes across STREAMTRAP and initializing models with this expanded class list (open-set). This setting is more representative of real-world deployments where practitioners may not have complete prior knowledge of which species are present at a given site. It also tests whether the adaptation recipe remains effective when the model must discriminate among a substantially larger set of candidate species.

Including rare species. As described in Sec. 3, rare species (fewer than 10 samples per interval) are excluded from evaluation to prevent severe class imbalance. However, rare species are often of greatest ecological interest, as they may include threatened or endangered populations that require urgent conservation attention. To reflect this, we include them exclusively in the test set, as they lack sufficient data

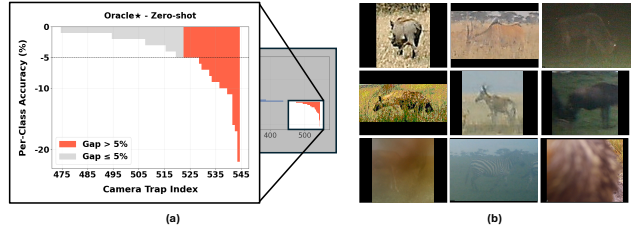


Figure A1. (a.) Detailed accuracy difference between oracle fine-tuning with our adaptation recipe (Oracle \star) and zero-shot (Fig. 4c). (b.) Qualitative examples of camera traps with severely degraded visual quality (e.g., blur, exposure artifacts, and sensor noise).

for a train/test split. This setup evaluates whether adapted models can still recognize species that were never or barely seen during training.

Results and analysis. The results in Tab. A4 indicate that all models perform worse under the open-set setting compared to the closed-set configuration, as the enlarged label space introduces additional confusion among visually similar species. Including rare species also degrades all models, but the oracle \star model suffers the largest drop, falling below both the zero-shot baseline and the accum \star model. We hypothesize that the oracle \star model over-adapts to dominant common classes across all pooled data, eroding the foundation model’s ability to recognize inherently rare species. The accum \star model, by adapting incrementally, better preserves general representations and remains competitive with the zero-shot baseline.

C.2. Remaining Failure Cases of Oracle \star

While our proposed approach generally improves the performance of the oracle models compared to the zero-shot baseline, 72 camera traps still underperform it (Fig. 4c). As illustrated in Fig. A1a, 48 of these 72 show a gap of at most 5%. However, the remaining 22 camera traps exhibit a more substantial degradation exceeding 5%. To better understand these limitations, we conduct a detailed analysis of these 22 camera traps, separating minor fluctuations from more systematic failure modes.

Poor image quality (5–10%). For the 16 camera traps with a moderate performance gap (between 5 and 10%), the degradation is primarily driven by poor image quality. To accurately mirror real-world deployment conditions, we intentionally retain low-quality images in which animals are present but difficult to discern. As illustrated in Fig. A1b, the animal is visible upon close inspection, yet the degraded image quality introduces noise that can mislead the fine-tuned model—whereas the zero-shot baseline, not having been exposed to these noisy training signals, remains unaffected. Filtering such low-quality images could improve overall model performance, but we consider this outside the current scope and leave it as a direction for future work.

Train–test distribution shift (>10%). For the 6 cam-

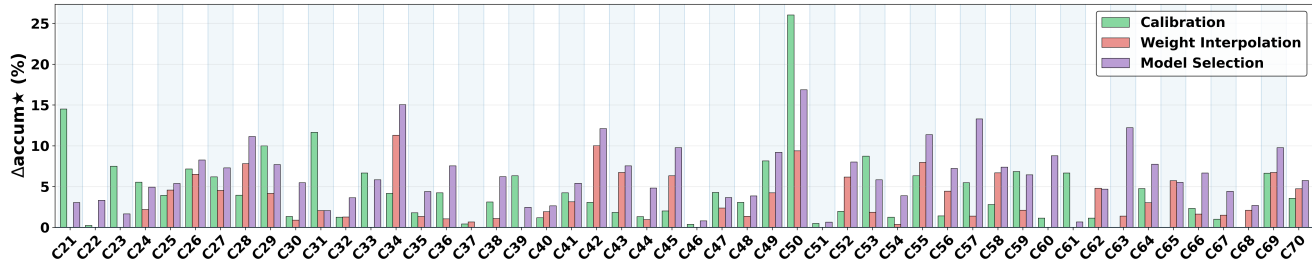


Figure A2. Performance gain (Δaccum^*) of calibration, weight interpolation, and model selection over the accum^* baseline across 50 cameras. They are applied on top of accum^* .

era traps exhibiting a performance drop of more than 10%, the degradation consistently traces back to a severe distribution shift between the training and test splits. As described in Sec. D.3, STREAMTRAP groups images from the same burst before splitting to reduce near-duplicate leakage across splits. While this makes the evaluation more realistic, it can also produce splits with markedly different visual conditions for some camera traps. For example, the training split may contain mostly daytime images, whereas the test split contains mostly nighttime images. Such a distribution mismatch appears to be the primary factor behind the largest failure cases, while the zero-shot baseline retains general knowledge that transfers across both conditions.

	Accuracy	ΔOracle^*
Oracle*	87.6	–
Accum*	78.8	8.8
+ Calibration	83.2	4.5
+ Weight Interpolation	82.0	5.7
+ Model Selection	85.1	2.5
+ Best Post-Processing	86.2	1.4

Table A5. Extended post-processing results by average per class accuracy (%). ΔOracle^* denotes remaining gap to Oracle* (87.6%). Each method is applied on top of Accum*. The blue row selects the best-performing post-processing method per camera trap.

C.3. Post-Processing: Extended Evaluation

To complement the post-processing analysis in Sec. 4.4, we evaluate all three post-processing methods on 50 additional camera traps where oracle* outperforms the zero-shot baseline, sampled to span a diverse range of accuracy gaps between the two models. As shown in Fig. A2 and Tab. A5, all methods yield promising improvements over the accum^* baseline, and selecting the best-performing post-processing method per camera trap further narrows the gap with oracle*. This suggests that with principled hyperparameter selection, post-processing can substantially boost adapted models. Developing automatic hyperparameter selection mechanisms that do not require access to future data remains a promising direction for future work.

C.4. Details of When Should We Adapt

As discussed in Sec. 5 and illustrated in Fig. 8, practitioners must decide whether to adapt the model when a new interval of data arrives. We construct an adapt-or-skip benchmark on top of STREAMTRAP to evaluate this. Throughout this section, we denote by model_j the model trained on cumulative labeled data from intervals $1, \dots, j$.

Experimental setup. Following the streaming protocol, at interval j , the learner has access to model_{j-1} and the unlabeled images from the current interval j . The learner must decide whether to:

- **Adapt:** label the interval j data and train model_j .
- **Skip:** continue using model_{j-1} .

This decision must be made *before observing the test data from interval $j + 1$* . The chosen model (either model_{j-1} or model_j) is then evaluated on the test split of interval $j + 1$. Each interval therefore, produces one adapt-or-skip decision instance. To construct the benchmark, we uniformly sample 80 camera traps from those where the oracle* performance exceeds the zero-shot baseline, and subsample decision instances to obtain a balanced dataset with equal numbers of Adapt and Skip cases. We evaluate three simple decision heuristics:

Random choice. Selects Adapt or Skip uniformly at random.

MSP-based confidence method. We compute the mean Maximum Softmax Probability (MSP) of model_j on the unlabeled images of interval j . The intuition is that model confidence can provide a coarse signal of distribution shift. Adaptation is triggered when the confidence falls below a threshold $\tau_{\text{MSP}}(j)$.

CLIP feature-distance method. We compute class prototypes using labeled data from intervals $1, \dots, j - 1$ in CLIP feature space. For images in interval j , we measure the ℓ_2 distance to the nearest class prototype and average across images. The intuition is that distribution shifts often manifest as changes in the representation space of a model. Adaptation is triggered when the mean distance exceeds threshold $\tau_{\text{feat}}(j)$.

Both thresholds are determined using statistics from the zero-shot model applied to the same unlabeled interval.



(a) Average Per-Class Accuracy of each method.



(b) Binary decision accuracy of each method.

Figure A3. Comparison of adapt-or-not methods on our balanced benchmark. Each interval is labeled as either a Skip case (where not adapting is correct) or an Adapt case (where adapting is correct), with Combined reporting overall accuracy across all intervals. Methods include Random, MSP-based, Feature-based, Always Adapt, Always Skip, and an Oracle upper bound. (a). Balanced accuracy under Skip, Adapt, and Combined evaluation. (b). Binary decision accuracy of each method.

Baselines. For context, we also include two non-decision baselines: *Always Adapt*, which updates the model at every interval, and *Always Skip*, which never adapts. We additionally report an *Oracle* upper bound that always selects the correct ground-truth action. The ground-truth action is defined as the choice (Adapt or Skip) that yields higher balanced accuracy on the test split of interval $j + 1$.

Evaluation metrics. We evaluate methods using two metrics: *Balanced Accuracy*, which measures the classification performance obtained by following the method’s decisions, and *Binary Decision Accuracy*, which measures the fraction of intervals where the method selects the correct action.

Results and analysis. Results are summarized in Fig. A3a and Fig. A3b. On cases where the ground-truth action is **Skip**, the oracle and *Always Skip* coincide (86.2%), while *Always Adapt* underperforms (65.3%). Conversely, in cases where the correct action is **Adapt**, the oracle and *Always Adapt* coincide (89.6%, while *Always Skip* falls to 64.6%. The three heuristic decision strategies perform close to random guessing. Their combined balanced accuracies (Random: 77.4%, MSP: 75.9%, Feature: 76.4%) are substantially below the oracle (87.8%). Binary decision accuracy shows a similar pattern, with MSP and Feature selecting the correct action only 47–48% of the time.

These results highlight that predicting when adaptation is beneficial remains a challenging and largely unexplored problem, motivating future research on more reliable adapt-or-not decision strategies.

C.5. More Camera Trap Results

Due to resource constraints, it is not feasible to conduct experiments across all 546 camera traps in STREAMTRAP for every setting. As such, Tab. A8 reports the camera traps for which experiments on all settings have been completed. Tab. A9 summarizes the camera trap index used throughout all figures and tables.

D. STREAMTRAP: Construction Details

D.1. Data Sources

The LILA BC repository hosts more than fifty datasets and continues to grow. As shown in Tab. A6, we limit the benchmark to a subset of camera trap datasets, excluding non-camera-trap sources such as sea-animal imagery, drone imagery, and geological or earth-observation images.

D.2. Data Processing Pipeline

The data processing pipeline is driven by a configuration file that specifies the target camera traps, the required filters, and various other experimental settings. Based on this configuration, the pipeline first retrieves and preprocesses the raw data.

Metadata preprocessing. All LILA BC camera trap datasets use the COCO camera trap format¹ metadata, which includes two optional fields—datetime and sequence—that are essential for our benchmark to group images into temporal intervals and to identify and handle burst images. When datetime is missing, we extract it from each image’s EXIF header² and insert it into the metadata if available; when sequence is missing, we generate pseudo-sequences by grouping neighboring images within 3 seconds of one another; and when both fields are absent, we first recover datetime from EXIF and then apply the sequence-grouping step. The above metadata preprocessing is implemented as a separate script due to the large amount of image downloading and long processing time it requires; however, it can be incorporated into the pipeline in the future to automatically handle newly added datasets with the same COCO-camera trap format.

¹A metadata standard maintained within the LILA BC repository, derived from the original COCO format.

²EXIF stands for Exchangeable Image File Format, a standard for storing metadata such as date and time inside image files.

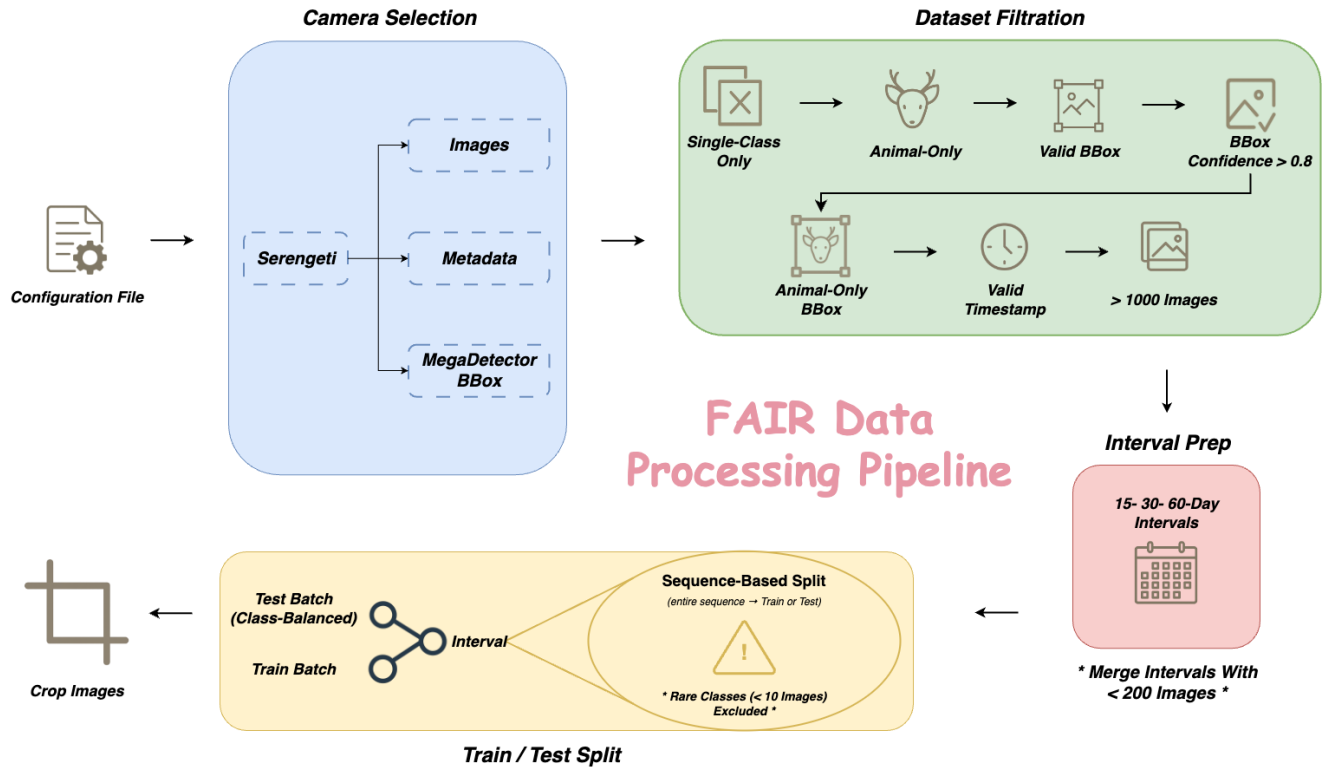


Figure A4. Detailed camera trap data processing pipeline. Raw camera trap images and metadata are filtered, temporally chunked, and cropped into standardized animal patches, producing per-camera chronological streams for online continual evaluation.

MegaDetector bounding box. During the initial preprocessing phase, the pipeline also checks the bounding box predictions to ensure they align with the preprocessed metadata. We use MegaDetector [4] v5a (MDv5a) as our unified detector across all datasets. MegaDetector evolves through multiple versions, each expanding its training corpus with both private and public camera trap datasets (e.g., Caltech Camera Traps [5], Snapshot Serengeti [46], WCS Camera Traps, NACTI [47], SWG Camera Traps [24]). MDv5a is trained on all MDv5b training data, along with additional public datasets such as iNaturalist 2017 [51] and COCO [27]. Prior evaluations report strong performance: WildEye reports that MDv5a achieves 99.2% animal recall at 97.26% precision, and ecological studies consistently report 90–98% recall and 92–99% precision across diverse environments.

Because several LILA BC datasets now include human-labeled bounding boxes (released after our benchmark preparation) and others still lack such annotations, we apply MDv5a uniformly to all 17 datasets to ensure consistent preprocessing. For datasets without human-labeled boxes, we rely entirely on MDv5a detections; for those with human labels, we still apply MDv5a with a high-confidence threshold for consistency. MDv5a outputs bounding boxes for animals, humans, and vehicles; we retain only animal detections and use metadata to link each bounding box to

its species. Our goal is not to study detection itself but to build a consistent and reliable foundation for classification.

Data processing. Once the initial data retrieval and metadata-detector matching are complete, the finalized data is passed through our processing pipeline, illustrated in Fig. A4. Applying the settings from the configuration file, the pipeline filters the data based on dataset or camera selection, minimum image count constraints, bounding-box confidence thresholds, and class exclusion for targeted taxa. Low-quality and other hard cases are filtered through these settings, enabling control over benchmark difficulty and data quality. This filtering step produces a substantial reduction in both images and camera traps, as summarized in Tab. A6, with 80.1% of images and 88.9% of camera traps filtered overall. This is largely driven by the prevalence of empty images: approximately 41.7% contain no animals. Such cases naturally arise in camera trap systems, where motion triggers frequently activate after animals leave the scene or due to minor environmental disturbances.

After removing non-informative images, the remaining valid data is grouped into temporal intervals, with a default window of 30-day chunks (adjustable to 15, 60, or custom durations). To ensure sufficient data for training and testing, we merge intervals when a chunk contains fewer than 200 images. Within each interval, the data is partitioned into training and testing sets. Crucially, this split is per-

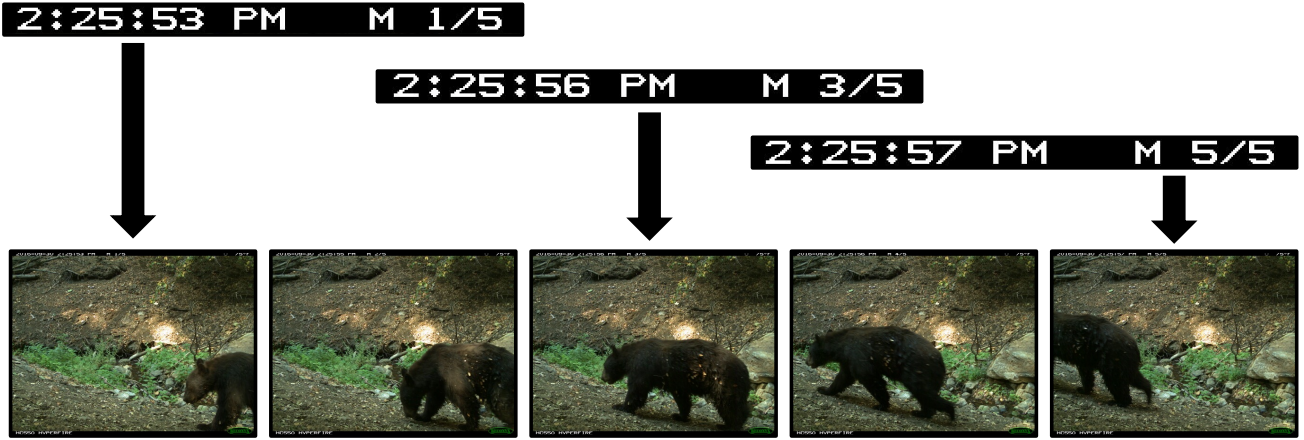


Figure A5. Illustration of burst images from a single sequence. Upon detecting motion, the camera captures multiple frames in rapid succession, producing images that share the same environment, background, and animal appearance.

formed while ensuring that burst images within the same sequence are kept in the same set to prevent temporal data leakage. While a fixed seed is not enforced by default, it can be specified to ensure reproducible splits, and rare class interval data may optionally be preserved alongside the training and test sets to support long-tail evaluation. Finally, the pipeline crops the actual images. Following prior work, we enlarge each detected region by 50% of the bounding box size before cropping. The pipeline then saves the prepared interval JSON data alongside these cropped patches as the final benchmark output for each camera trap. The processed camera trap list is summarized in Tab. A7.

D.3. One Trigger, Multiple Frames: Burst Images

Camera trap devices capture bursts of images when motion is detected, with each burst containing 3 to over 10 frames, which we refer to as a *sequence*. Using sequence IDs and frame-order metadata, we assign all frames from each sequence to a single split (train or test). As shown in Fig. A5, frames within a sequence are captured within seconds and depict the same animal, resulting in extremely high visual correlation. Splitting such frames across train and test would therefore introduce temporal leakage, artificially inflating performance. To avoid this, we enforce strict sequence-level splitting.

While splits are defined at the sequence level, each image is treated as an independent training and evaluation sample. We acknowledge that explicitly modeling intra-sequence correlations may further improve performance, but it is beyond our current scope. Moreover, evaluating at the sequence level, via single-frame downsampling or aggregating predictions across sequences, could provide a more realistic setting. Quantifying the resulting dataset size reduction and performance shifts remains an important direction for future work.

Dataset	Continent	Original Dataset			STREAMTRAP		
		# Img	# Cls	# Traps	# Img	# Cls	# Traps
Caltech Camera Traps [5]	N. America	243.1K	22	140	37.6K	13	15
Idaho Camera Traps [23]	N. America	1535.7K	62	276	43.6K	10	15
NA Camera Trap Img [47]	N. America	3280.8K	59	551	964.9K	20	52
NZ Trail Cam. Animals [33]	Oceania	2045.8K	98	2469	543.9K	41	139
Orinoquía Camera Traps [53]	S. America	112.2K	58	49	20.1K	16	6
Snapshot APNR* [35]	Africa	228.4K	60	148	102.2K	19	40
Snapshot Camdeboo* [35]	Africa	67.6K	48	59	22.9K	23	12
Snapshot Enonkishu* [35]	Africa	132.8K	48	83	59.7K	23	13
Snapshot Karoo* [35]	Africa	261.7K	48	96	21.2K	17	10
Snapshot Kgalagadi* [35]	Africa	94.7K	48	132	23.6K	16	9
Snapshot Kruger* [35]	Africa	59.6K	59	124	5.8K	11	3
Snapshot Madikwe* [35]	Africa	277.5K	69	136	122.1K	28	28
Snapshot Mt. Zebra* [35]	Africa	412.4K	59	74	15.4K	21	7
Snapshot Pilanesberg* [35]	Africa	108.7K	65	65	13.3K	19	3
Snapshot Ruaha* [35]	Africa	351.0K	54	47	4.6K	13	2
Snapshot Serengeti [46]	Africa	7178.4K	61	225	1308.4K	45	188
Wellington Cam. Traps [3]	Oceania	270.5K	17	215	8.1K	7	4

Table A6. Summary of dataset statistics from the selected original LILA BC sources and STREAMTRAP after applying the proposed data processing and filtering pipeline. Datasets marked with * indicate datasets grouped under the unified project *Snapshot Safari 2024 Expansion* [35]. Image counts are reported in thousands (K) with one-decimal precision.

Table A7. Per-camera-trap statistics for all 546 camera traps in STREAMTRAP, grouped by dataset. Each entry lists the camera trap ID, total image count, number of time intervals, and number of species classes.

Name	Images	Int.	Cls.	Name	Images	Int.	Cls.
Caltech Camera Traps (15 camera traps)							
23	1,749	8	7	57	3,951	11	7
100	2,721	10	7	33	1,614	7	7
61	1,245	6	6	106	1,626	8	7
38	5,038	12	7	70	2,568	10	7
114	4,896	10	9	43	1,903	8	7
76	3,376	11	6	115	1,437	6	8
46	2,463	10	7	88	1,755	8	8
120	1,208	6	5				
Idaho Camera Traps (15 camera traps)							
84	2,545	7	7	94	2,048	8	6
117	2,023	7	5	85	2,299	9	5
98	3,380	7	5	118	3,191	10	6
86	3,120	10	7	100	4,865	8	7
121	4,427	11	6	87	1,692	7	5
105	1,354	6	5	122	4,319	10	6
89	4,562	10	5	109	1,356	6	6
124	2,430	6	8				
NA Camera Trap Images (52 camera traps)							
archbold_FL-01	51,120	12	5	archbold_FL-43	5,116	8	6
lebec_CA-19	7,965	11	12	archbold_FL-04	21,313	16	6
archbold_FL-44	2,776	9	6	lebec_CA-20	20,483	14	11
archbold_FL-05	30,121	14	8	lebec_CA-01	5,867	11	11
lebec_CA-21	4,270	12	13	archbold_FL-09	48,065	10	8
lebec_CA-02	8,827	16	11	lebec_CA-24	9,246	15	12
archbold_FL-15	11,817	14	8	lebec_CA-03	15,426	14	12
lebec_CA-26	6,997	12	12	archbold_FL-16	80,565	14	8
lebec_CA-04	14,661	17	12	lebec_CA-27	13,616	15	12
archbold_FL-19	42,460	14	7	lebec_CA-05	2,929	13	11
lebec_CA-29	34,320	16	10	archbold_FL-20	22,038	14	6
lebec_CA-06	12,450	18	12	lebec_CA-30	41,674	18	12
archbold_FL-23	15,533	14	9	lebec_CA-07	11,005	16	11
lebec_CA-31	13,549	15	9	archbold_FL-26	13,765	13	7
lebec_CA-09	5,597	15	11	lebec_CA-32	3,730	9	9
archbold_FL-28	35,480	15	5	lebec_CA-10	17,806	17	12
lebec_CA-36	3,258	11	10	archbold_FL-30	26,237	14	5
lebec_CA-11	13,471	14	12	lebec_CA-37	27,415	15	10
archbold_FL-31	35,364	15	6	lebec_CA-12	11,502	14	10
lebec_CA-38	22,459	18	13	archbold_FL-37	16,756	11	8
lebec_CA-13	8,598	14	9	lebec_CA-40	4,054	11	14
archbold_FL-38	21,583	11	9	lebec_CA-14	7,512	17	12
lebec_CA-41	18,323	17	11	archbold_FL-39	5,973	10	8
lebec_CA-16	3,811	12	12	lebec_CA-45	12,950	10	10
archbold_FL-41	21,502	11	6	lebec_CA-17	34,437	19	11
archbold_FL-42	8,783	9	5	lebec_CA-18	30,290	18	10
NZ Trail Cam Animals (139 camera traps)							
DWT_BCAM419_2022_1	11,216	6	8	EFD_DCAMH02	1,456	6	6
EFH_HCAME08	5,117	12	8	DWT_BCAM668_2022_1	2,873	6	7
EFD_DCAMH04	1,179	6	9	EFH_HCAME09	3,758	11	8
EFD_DCAMA02	1,683	7	7	EFD_DCAMH06	3,924	12	9

Continued on next page...

Name	Images	Int.	Cls.	Name	Images	Int.	Cls.
EFH_HCAME10	4,730	14	11	EFD_DCAMA04	2,969	13	10
EFD_DCAMH07	1,143	6	7	EFH_HCAMF01	4,339	14	12
EFD_DCAMA05	2,636	10	5	EFD_DCAMH08	3,220	9	5
EFH_HCAMF02	9,138	19	17	EFD_DCAMA06	2,736	11	8
EFD_DCAMH09	1,169	6	7	EFH_HCAMF04	4,909	17	15
EFD_DCAMA07	2,021	8	5	EFH_HCAMA02	4,543	8	10
EFH_HCAMF07	2,288	7	11	EFD_DCAMA08	2,268	9	9
EFH_HCAMA03	2,612	7	8	EFH_HCAMF09	9,324	21	17
EFD_DCAMA10	1,310	6	11	EFH_HCAMA05	6,954	10	7
EFH_HCAMF11	1,918	9	13	EFD_DCAMA11	1,605	7	9
EFH_HCAMA06	6,065	10	10	EFH_HCAMF12	2,310	9	11
EFD_DCAMB02	3,577	12	11	EFH_HCAMA07	5,350	13	7
EFH_HCAMG07	4,249	13	15	EFD_DCAMB03	2,276	8	6
EFH_HCAMA09	8,531	10	6	EFH_HCAMG08	2,416	11	10
EFD_DCAMB04	2,115	6	7	EFH_HCAMA10	5,290	8	10
EFH_HCAMG10	2,298	9	9	EFD_DCAMB06	2,645	8	6
EFH_HCAMA12	4,563	7	5	EFH_HCAMG12	16,709	19	15
EFD_DCAMB07	2,963	10	9	EFH_HCAMA13	1,908	7	6
EFH_HCAMG13	4,044	16	16	EFD_DCAMC02	2,422	9	8
EFH_HCAMB01	2,806	8	6	EFH_HCAMG14	1,910	7	10
EFD_DCAMC03	3,568	10	8	EFH_HCAMB02	2,898	9	5
EFH_HCAMG15	3,676	12	14	EFD_DCAMC04	3,378	7	8
EFH_HCAMB03	3,973	11	7	EFH_HCAMH02	4,148	8	7
EFD_DCAMC05	1,861	6	6	EFH_HCAMB04	5,767	13	5
EFH_HCAMH03	3,239	7	11	EFD_DCAMC07	1,700	7	8
EFH_HCAMB05	2,086	7	8	EFH_HCAMH04	4,209	8	9
EFD_DCAMC08	2,535	10	7	EFH_HCAMB07	6,675	14	10
EFH_HCAMH05	5,167	12	7	EFD_DCAMC09	1,609	7	6
EFH_HCAMB08	6,292	12	12	EFH_HCAMH06	6,766	12	10
EFD_DCAMC10	2,933	10	9	EFH_HCAMB09	4,124	12	11
EFH_HCAMH07	2,429	7	5	EFD_DCAMD02	2,648	10	10
EFH_HCAMB10	3,024	7	9	EFH_HCAMH08	3,779	8	7
EFD_DCAMD03	3,386	10	7	EFH_HCAMB11	1,667	6	7
EFH_HCAMH09	2,356	6	9	EFD_DCAMD04	3,238	11	7
EFH_HCAMC01	3,711	6	8	EFH_HCAMI01	2,985	6	8
EFD_DCAMD06	3,185	11	9	EFH_HCAMC02	5,822	11	7
EFH_HCAMJ01	4,264	9	6	EFD_DCAMD07	3,164	11	11
EFH_HCAMC03	7,002	11	6	EFH_HCAMJ02	4,660	6	6
EFD_DCAMD08	1,421	6	8	EFH_HCAMC04	7,950	12	10
EFH_HCAMJ04	3,451	8	6	EFD_DCAMD10	2,408	9	6
EFH_HCAMC06	5,657	12	9	EFH_HCAMJ06	3,176	7	6
EFD_DCAMD11	1,591	7	7	EFH_HCAMC07	6,136	13	10
HLO_HPAT003	1,336	7	6	EFD_DCAME01	2,734	11	13
EFH_HCAMC08	3,137	7	9	HLO_Moto2	2,257	9	6
EFD_DCAME02	2,664	6	10	EFH_HCAMD01	3,048	6	8
PS1_CAM6213	1,808	6	5	EFD_DCAME03	3,920	13	13
EFH_HCAMD03	2,382	8	5	PS1_CAM6604	1,698	7	5
EFD_DCAME04	2,922	11	13	EFH_HCAMD04	6,641	12	12
PS1_CAM6803	3,567	7	6	EFD_DCAME06	3,940	13	12
EFH_HCAMD05	4,442	8	8	PS1_CAM6808	1,701	7	5
EFD_DCAME07	6,248	15	12	EFH_HCAMD06	3,400	10	11
PS1_CAM7312	1,545	6	6	EFD_DCAME08	6,165	14	12
EFH_HCAMD07	5,754	11	10	PS1_CAM7709	2,103	6	5
EFD_DCAME09	2,169	7	10	EFH_HCAMD08	4,996	13	12
PS1_CAM7811	2,955	6	6	EFD_DCAMF02	1,414	6	8

Continued on next page. . .

Name	Images	Int.	Cls.	Name	Images	Int.	Cls.
EFH_HCAMD09	3,652	9	9	PS1_CAM7816	4,961	7	6
EFD_DCAMF03	6,737	18	12	EFH_HCAMD10	2,178	6	9
PS1_CAM7920	3,099	8	5	EFD_DCAMF06	3,950	13	10
EFH_HCAME02	11,502	16	10	PS1_CAM8001	1,823	6	7
EFD_DCAMF07	10,160	19	10	EFH_HCAME03	11,811	15	9
PS1_CAM8008	1,808	6	8	EFD_DCAMF08	4,313	15	14
EFH_HCAME04	8,765	15	12	PS1_CAM8306	1,342	6	5
EFD_DCAMF09	7,199	21	18	EFH_HCAME05	4,372	10	6
ZIO_TRAILCAM01	5,918	6	5	EFD_DCAMG03	2,576	11	6
EFH_HCAME06	3,061	11	8	EFD_DCAMH01	1,394	6	8
EFH_HCAME07	5,113	14	8				
Orinoquía Camera Traps (6 camera traps)							
M00	2,028	6	11	N04	1,403	6	9
N25	3,188	6	7	M04	5,931	6	7
N07	1,759	6	7	N29	5,820	6	10
Snapshot APNR (40 camera traps)							
6U	2,081	10	8	K044	2,621	14	6
TB17	5,461	15	12	13U	6,329	23	9
K051	1,747	9	8	TB26	5,768	17	10
BOSP	1,759	6	6	K053	1,596	8	8
U23A	1,429	7	8	JJ5	4,560	21	9
K062	1,188	6	7	U24B	1,560	8	7
JJ6	3,223	16	10	K064	2,097	10	7
U43B	1,743	9	6	JJ7	3,229	17	8
K082	2,042	11	9	U63C	3,108	14	8
JJP	4,910	23	12	KUMH	1,297	6	6
U64C	2,536	12	12	K011	1,837	9	7
LL5	1,604	8	12	UMH8	1,846	9	9
K013	2,322	12	6	N1	1,449	8	10
UMH9	3,691	18	10	K021	2,264	11	9
N3	1,126	6	6	WB4	2,098	11	8
K023	2,737	15	12	N5	1,450	7	9
WM	2,201	11	6	K024	3,755	17	11
RM4	1,640	8	7	WS6	1,636	7	8
K034	2,843	15	10	TB12	1,920	9	9
K041	1,914	10	8	TB14	3,548	16	10
Snapshot Camdeboo (12 camera traps)							
A05	2,924	11	10	B07	1,948	9	11
D03	2,901	12	8	A06	1,866	8	11
C06	3,226	12	9	D04	1,314	6	8
B04	1,666	8	8	C07	1,626	8	13
D06	1,086	6	9	B06	1,374	7	11
D02	1,510	7	7	E02	1,461	6	8
Snapshot Enonkishu (13 camera traps)							
B02	1,855	6	10	C03	2,858	12	9
D04	2,115	8	9	B03	1,358	8	7
C04	6,271	16	14	D06	8,572	19	11
B05	4,869	10	13	C05	8,413	13	12
E06	7,247	17	10	B06	7,601	13	11
C06	3,123	11	13	C02	2,724	12	13
D01	2,710	12	14				
Snapshot Karoo (10 camera traps)							
A01	1,951	9	10	C01	4,647	15	11

Continued on next page...

Name	Images	Int.	Cls.	Name	Images	Int.	Cls.
E03	1,383	7	7	A02	2,533	12	11
D01	1,245	6	10	F03	1,349	6	11
B02	3,030	11	10	D04	1,538	8	11
B03	1,941	6	11	E01	1,540	8	9
Snapshot Kgalagadi (9 camera traps)							
KHOGA04	1,568	7	7	KHOGB06	3,118	11	9
KHOLA03	2,158	7	7	KHOGB03	3,612	10	9
KHOGB07	3,406	11	9	KHOLA05	2,805	10	5
KHOGB04	1,847	7	7	KHOGC05	1,561	7	9
KHOLA08	3,533	10	5				
Snapshot Kruger (3 camera traps)							
7	2,679	10	11	8	1,482	6	7
49	1,616	8	9				
Snapshot Madikwe (28 camera traps)							
A03	2,064	9	7	D03	1,743	9	8
I05	2,250	9	7	A04	1,886	9	9
D04	1,304	7	8	I06	2,987	10	8
A05	3,536	12	10	D07	3,699	15	9
I08	1,347	7	10	A06	1,603	8	6
F03	1,254	6	5	MAD01	10,599	11	15
B03	1,928	8	8	F04	1,515	7	7
MAD03	21,236	10	14	B05	5,837	13	9
G04	2,107	10	10	MAD04	10,580	11	15
B06	1,444	7	9	G05	1,481	7	7
MAD05	4,488	11	12	C04	5,867	15	10
G08	1,757	8	8	MAD06	16,721	11	14
C06	6,992	14	8	H08	1,556	9	10
C07	2,522	11	8	I04	1,771	9	12
Snapshot Mt. Zebra (7 camera traps)							
B04	1,230	6	7	D06	1,402	7	6
F05	4,870	13	6	C08	1,691	9	11
E05	1,891	9	11	D03	2,472	11	17
F04	1,864	9	8				
Snapshot Pilanesberg (3 camera traps)							
B04	4,555	11	12	C02	3,578	8	16
D01	5,182	11	12				
Snapshot Ruaha (2 camera traps)							
M2	2,824	8	12	M7	1,814	6	8
Snapshot Serengeti (188 camera traps)							
B03	7,120	21	14	G10	2,403	11	12
M09	16,681	30	21	B04	3,206	16	9
G12	2,790	11	14	M13	3,924	10	10
B05	6,125	23	14	G13	1,586	6	6
N02	2,177	6	10	B06	9,245	28	20
H01	8,037	29	17	N04	3,826	16	15
B07	19,353	24	13	H02	24,145	40	19
N05	7,955	23	15	B08	10,969	21	11
H03	5,021	26	14	N06	12,734	35	18
B09	7,194	16	8	H04	12,146	28	11
N08	10,528	27	16	B10	3,609	14	13
H05	19,184	39	15	N09	11,525	30	16
B12	1,805	8	11	H08	5,555	16	14

Continued on next page...

Name	Images	Int.	Cls.	Name	Images	Int.	Cls.
N10	7,505	8	14	B13	7,484	25	13
H09	1,715	9	9	N12	1,427	7	10
C01	20,361	26	14	H11	4,705	14	12
O04	2,403	8	12	C02	13,935	36	13
H13	5,488	15	15	O05	7,921	15	13
C03	6,346	20	13	I01	6,483	26	14
O06	9,362	33	18	C04	11,480	20	13
I02	7,109	30	18	O07	7,806	24	17
C05	9,558	21	14	I03	12,020	30	16
O08	6,279	19	17	C06	7,610	22	13
I04	8,834	32	12	O09	7,334	18	15
C07	13,071	23	14	I05	11,945	25	14
O10	8,033	22	13	C08	15,194	29	12
I06	7,830	23	12	O11	2,017	9	10
C10	7,380	16	13	I07	5,770	16	15
O13	2,247	7	7	C11	8,223	16	17
I08	3,845	15	16	P03	6,328	8	15
C12	8,509	20	8	I11	5,708	15	11
P04	3,629	9	13	C13	19,272	29	14
I12	2,778	13	14	P05	11,115	20	17
D02	16,352	32	13	I13	6,575	18	20
P06	7,446	18	14	D03	15,148	36	12
J01	1,346	7	11	P07	5,415	17	15
D04	10,382	31	14	J02	8,168	27	16
P09	7,397	13	8	D05	4,025	11	11
J03	11,000	30	17	P10	12,014	33	19
D06	12,254	19	16	J04	9,206	24	12
P11	2,556	9	14	D07	1,906	8	9
J05	13,050	34	18	P13	7,626	20	12
D08	5,013	14	10	J06	8,182	23	10
Q04	2,188	8	12	D09	5,927	16	14
J07	2,361	10	11	Q05	4,947	19	15
D10	3,003	8	12	J08	3,286	16	16
Q06	5,622	17	12	D11	6,295	18	14
J09	7,166	25	17	Q07	6,497	23	14
D12	2,733	11	10	J10	3,946	13	15
Q08	7,799	25	14	D13	4,208	14	10
J12	9,840	28	19	Q09	2,981	8	15
E01	4,873	18	16	J13	2,907	12	13
Q10	1,807	9	10	E02	17,938	29	20
K03	11,493	29	17	Q11	4,503	16	9
E03	13,175	36	18	K04	7,131	25	12
Q12	4,731	14	11	E04	15,297	38	15
K05	3,346	12	11	Q13	2,507	7	7
E05	8,331	32	15	K06	11,903	24	13
R05	2,799	6	12	E06	11,219	19	17
K07	8,676	22	18	R06	5,058	13	13
E08	3,704	8	11	K08	3,380	15	12
R08	5,616	16	9	E09	7,750	21	21
K09	10,019	17	20	R09	8,602	23	12
E12	4,930	7	12	K10	2,183	10	9
R10	3,431	6	11	E13	5,915	19	14
K11	1,311	7	10	R11	1,892	8	9
F01	5,808	23	14	K12	1,435	6	6
R12	3,548	10	7	F02	7,012	27	13

Continued on next page. . .

Name	Images	Int.	Cls.	Name	Images	Int.	Cls.
K13	4,340	6	12	S07	1,863	8	8
F03	3,426	15	15	L02	1,170	6	8
S08	1,763	10	12	F04	3,217	13	14
L03	4,556	16	12	S09	10,328	30	15
F05	9,555	16	17	L04	3,728	11	14
S10	4,918	13	8	F06	4,458	13	12
L05	10,006	18	17	S11	15,134	25	17
F07	2,679	13	10	L06	3,454	13	11
S13	3,507	11	12	F08	2,696	12	12
L07	4,852	15	13	T08	2,968	10	12
F09	2,009	7	15	L08	8,799	21	15
T09	3,808	15	14	F10	8,906	17	20
L09	2,934	9	12	T10	11,036	28	12
F12	2,963	9	13	L10	9,520	26	18
T11	13,764	28	16	F13	2,392	6	7
L11	2,958	11	12	T12	8,805	21	10
G01	6,697	23	13	M02	1,118	6	11
T13	7,477	11	13	G02	9,028	27	17
M03	1,470	6	15	U09	8,125	17	14
G03	6,707	20	15	M04	4,319	14	14
U10	14,568	24	16	G04	8,262	27	13
M05	10,845	18	18	U12	3,735	12	9
G05	7,356	20	14	M06	10,034	23	18
U13	4,340	9	17	G06	1,737	9	9
M07	9,756	19	18	V10	6,393	15	14
G07	8,758	22	17	M08	8,176	22	12
Wellington Camera Traps (4 camera traps)							
031c	1,696	6	5	235	2,916	8	5
046c	1,834	6	5	324	1,697	6	5

	C1	C2	C3	C4	C5	C6	C7	C8	C9	C10	C11	C12	C13	C14	C15	C16	C17	C18	C19	C20	C21	C22	C23	C24	C25	C26	C27	C28	C29	C30	C31	C32	C33	C34	C35	C36	C37	C38	C39	Avg.
ZS	94.1	97.7	81.3	94.5	75.8	81.5	85.6	80.1	81.2	62.7	79.3	75.3	69.5	87.2	82.6	76.5	92.3	77.9	80.2	82.1	66.0	58.3	64.1	77.1	79.1	85.3	72.0	67.6	69.6	79.0	84.3	63.2	56.3	79.7	90.9	75.5	90.9	75.8	55.8	77.6
Accum	63.2	73.6	56.0	72.9	57.0	50.0	75.7	60.0	73.0	60.6	76.0	66.0	66.0	75.1	68.0	68.0	77.1	73.0	74.0	72.0	11.4	16.7	26.0	25.0	25.0	26.3	20.0	25.0	16.7	33.3	33.3	39.7	33.3	27.1	50.0	38.0	53.6	42.5	45.7	49.9
Δ	30.9	24.1	25.3	21.6	18.8	31.5	9.9	20.1	8.2	2.1	3.3	9.3	3.5	12.1	14.6	8.5	15.2	4.9	6.2	10.1	54.6	41.6	38.1	52.1	54.1	59.0	52.0	42.6	52.9	45.7	51.0	23.5	23.0	52.6	40.9	37.5	37.3	33.3	10.1	-
Accum*	98.0	98.7	79.6	94.7	76.9	69.7	94.5	75.9	88.3	75.4	90.7	80.0	79.6	88.2	81.0	80.9	89.9	84.9	85.4	83.0	76.6	79.3	81.0	78.7	78.1	79.1	72.7	75.0	66.4	82.2	79.2	83.4	76.7	70.3	89.9	77.2	92.2	79.4	82.6	81.9
Δ	3.9	1.0	1.7	0.2	1.1	11.8	8.9	4.2	7.1	12.7	11.4	4.7	10.1	1.0	1.6	4.4	2.4	7.0	5.2	0.9	10.6	21.0	16.9	1.6	1.0	6.2	0.7	7.4	3.2	3.2	5.1	20.2	20.4	9.4	1.0	1.7	1.3	3.6	26.8	-
Oracle*	96.1	98.7	84.9	96.5	84.3	82.2	90.0	81.6	91.0	89.7	92.1	82.4	78.7	90.3	87.8	87.0	96.4	91.6	87.8	86.8	83.9	81.4	89.9	82.0	84.0	87.7	79.8	85.0	87.0	86.9	91.5	84.7	89.9	87.9	94.5	81.3	95.8	83.3	93.4	87.8
Δ	2.0	1.0	3.6	2.0	8.5	0.7	4.4	1.5	9.8	27.0	12.8	7.1	9.2	3.1	5.2	10.5	4.1	13.7	7.6	4.7	17.9	23.1	25.8	4.9	4.9	2.4	7.8	17.4	17.4	7.9	7.2	21.5	33.6	8.2	3.6	5.8	4.9	7.5	37.6	-
C40	C41	C42	C43	C44	C45	C46	C47	C48	C49	C50	C51	C52	C53	C54	C55	C56	C57	C58	C59	C60	C61	C62	C63	C64	C65	C66	C67	C68	C69	C70	C71	C72	C73	C74	C75	C76	C77	C78	C79	Avg.
ZS	77.5	78.3	81.0	86.1	83.0	78.9	62.2	81.5	80.9	78.3	66.0	67.1	73.8	56.9	89.1	74.7	83.1	69.8	61.5	59.8	70.1	72.2	80.4	66.7	71.4	64.7	89.0	76.6	58.6	85.7	81.6	60.6	61.8	70.4	67.0	70.8	78.4	79.3	74.8	73.6
Accum	50.0	45.0	36.8	46.7	54.2	50.0	61.7	56.7	72.3	56.2	45.0	66.7	50.0	71.7	54.0	62.5	60.8	58.0	64.3	68.2	72.3	71.0	54.3	63.9	56.9	62.3	70.9	66.6	90.0	96.7	79.2	64.2	65.7	61.4	75.8	71.5	79.3	67.5	63.4	
Δ	27.5	33.3	44.2	39.4	28.8	28.9	0.5	24.8	8.6	22.1	21.0	0.4	23.8	6.9	17.4	20.7	20.6	9.0	3.5	4.5	1.9	0.1	9.4	12.4	7.5	7.8	26.7	5.7	8.0	4.3	15.1	18.6	2.4	4.7	5.6	5.0	6.9	0.0	7.3	-
Accum*	86.2	81.0	71.8	79.4	86.4	78.3	88.9	83.4	87.2	77.7	66.5	86.9	70.1	70.0	90.8	71.8	79.5	75.4	71.3	75.7	79.4	83.3	83.5	81.6	72.6	65.3	86.6	77.9	68.7	82.1	81.5	87.6	84.2	86.8	61.5	79.8	88.5	89.3	76.7	79.4
Δ	8.7	2.7	9.2	6.7	3.4	0.6	26.7	1.9	6.3	0.6	0.5	19.8	3.7	13.1	1.7	2.9	3.6	5.6	9.8	15.9	9.3	11.1	3.1	14.9	1.2	0.6	2.4	1.3	10.1	3.6	0.1	27.0	22.4	16.4	5.5	9.0	10.1	10.0	1.9	-
Oracle*	89.4	87.3	83.4	87.8	96.3	84.8	93.8	91.0	91.9	84.1	91.3	91.0	88.5	85.4	96.6	84.3	89.9	86.6	89.6	80.4	91.0	93.3	91.9	91.6	86.4	70.3	91.9	87.4	79.4	88.6	86.9	96.7	86.9	90.2	83.8	84.8	90.7	91.9	88.2	88.3
Δ	11.9	9.0	2.4	1.7	13.3	5.9	31.6	9.5	11.0	5.8	25.3	23.9	14.7	28.5	7.5	9.6	6.8	16.8	28.1	20.6	20.9	21.1	11.5	24.9	15.0	5.6	2.9	10.8	20.8	2.9	5.3	36.1	25.1	19.8	16.8	14.0	12.3	12.6	13.4	-
C79	C80	C81	C82	C83	C84	C85	C86	C87	C88	C89	C90	C91	C92	C93	C94	C95	C96	C97	C98	C99	C100	C101	C102	C103	C104	C105	C106	C107	C108	C109	C110	C111	C112	C113	C114	C115	C116	Avg.		
ZS	66.7	75.6	63.6	82.4	79.8	71.2	82.0	84.7	73.9	71.9	75.6	88.3	90.2	87.7	89.9	86.8	89.6	92.8	87.7	74.8	88.0	91.3	91.9	93.4	93.4	78.9	84.6	95.8	93.9	95.9	98.0	96.3	93.3	97.3	94.1	90.7	94.0	95.8	86.4	
Accum	64.8	79.0	56.0	78.5	61.8	75.5	83.5	65.4	66.2	73.3	83.2	78.1	88.3	82.7	69.1	84.7	88.0	72.2	69.5	77.0	70.8	83.0	81.0	78.0	84.5	81.1	71.4	82.0	76.8	81.3	53.6	62.3	89.4	90.4	78.2	64.2	81.7	75.8		
Δ	1.9	3.4	7.6	3.9	4.0	9.4	6.5	1.2	8.5	5.7	2.3	5.1	12.1	0.6	7.2	17.7	4.9	4.8	15.5	5.3	11.0	20.5	8.9	12.4	15.4	5.6	3.5	24.4	11.9	19.1	16.7	42.7	31.0	7.9	3.7	12.5	29.8	14.1	-	
Accum*	77.3	70.0	33.4	90.3	88.4	81.5	88.1	85.5	61.6	78.2	80.4	90.9	94.4	90.8	92.5	84.8	93.2	92.8	87.0	74.2	90.2	92.5	88.1	93.8	94.2	91.1	86.0	96.7	93.1	95.9	98.9	95.8	92.9	97.7	90.2	88.1	92.0	95.1	87.0	
Δ	10.6	5.6	30.2	7.9	8.6	10.3	6.1	0.8	12.3	6.3	4.8	2.6	4.2	3.1	2.6	2.0	3.6	0.0	0.7	0.6	2.2	1.2	3.8	0.4	0.8	12.2	1.4	0.9	0.8	0.0	0.9	0.5	0.4	0.4	3.9	2.6	2.0	0.7	-	
Oracle*	79.6	88.5	76.3	93.4	91.2	80.1	91.3	94.0	83.2	80.4	83.0	95.2	95.6	94.0	95.9	91.9	94.8	98.4	92.0	79.4	92.4	95.0	95.5	96.5	96.9	82.6	87.7	98.3	95.7	98.3	99.8	97.8	94.9	98.2	94.9	92.4	94.3	96.3	91.7	
Δ	12.9	12.9	12.7	11.0	11.4	8.9	9.3	9.3	8.5	7.4	6.9	5.4	6.3	6.0	5.1	5.2	5.6	4.3	4.6	4.4	3.7	3.6	3.1	3.5	3.7	3.1	2.5	1.8	2.4	1.8	1.5	1.6	0.9	0.8	1.7	0.3	0.5	-		

Table A8. Complete result of ZS, Oracle*, Accum, Accum*. Blue (red) denotes improvement (degradation) relative to ZS.

Table A9. Camera trap index. Each camera trap is assigned an index C_i (e.g., C_1 , C_2) used to reference camera traps in figures and tables throughout the paper.

Index	Dataset	Camera Trap	Index	Dataset	Camera Trap
C1	Snapshot APNR	13U	C59	NZ Trail Cam. Animals	EFH_HCAME07
C2	Snapshot APNR	K082	C60	NZ Trail Cam. Animals	EFH_HCAMB04
C3	Snapshot Serengeti	Q09	C61	NZ Trail Cam. Animals	EFD_DCAMB04
C4	Snapshot Mt. Zebra	E05	C62	NZ Trail Cam. Animals	EFD_DCAME09
C5	Snapshot Serengeti	Q10	C63	NZ Trail Cam. Animals	EFD_DCAME05
C6	NZ Trail Cam. Animals	EFH_HCAMI01	C64	NZ Trail Cam. Animals	EFH_HCAMB07
C7	Caltech Camera Trap	88	C65	Orinoquía Camera Traps	M04
C8	Snapshot Serengeti	K11	C66	NZ Trail Cam. Animals	EFD_DCAME03
C9	Snapshot Enonkishu	C02	C67	Snapshot Kgalagadi	KHOGC05
C10	Snapshot Kgalagadi	KHOLA03	C68	Orinoquía Camera Traps	N29
C11	NZ Trail Cam. Animals	EFH_HCAME09	C69	Snapshot Serengeti	B04
C12	Snapshot Serengeti	L10	C70	NZ Trail Cam. Animals	EFD_DCAME03
C13	Snapshot Serengeti	L06	C71	NZ Trail Cam. Animals	PS1_CAM6213
C14	Snapshot Madikwe	H08	C72	NZ Trail Cam. Animals	EFH_HCAMD05
C15	Snapshot Serengeti	D09	C73	NZ Trail Cam. Animals	EFD_DCAME04
C16	NZ Trail Cam. Animals	EFH_HCAMD08	C74	Snapshot Serengeti	C08
C17	NA Camera Trap Img	lebec_CA-19	C75	NZ Trail Cam. Animals	EFH_HCAME02
C18	NZ Trail Cam. Animals	EFH_HCAME08	C76	Snapshot Madikwe	A05
C19	Snapshot Serengeti	H11	C77	Snapshot Madikwe	D03
C20	NZ Trail Cam. Animals	EFD_DCAME06	C78	NZ Trail Cam. Animals	EFH_HCAME02
C21	NZ Trail Cam. Animals	EFH_HCAME03	C79	Snapshot Serengeti	B10
C22	NZ Trail Cam. Animals	EFH_HCAMB10	C80	Snapshot Serengeti	I01
C23	NZ Trail Cam. Animals	EFH_HCAMD10	C81	Snapshot Serengeti	E09
C24	Snapshot Serengeti	M13	C82	Snapshot Serengeti	I11
C25	Snapshot Serengeti	D12	C83	NZ Trail Cam. Animals	EFH_HCAMD07
C26	Snapshot Serengeti	L04	C84	Orinoquía Camera Traps	N25
C27	Snapshot Serengeti	O04	C85	Snapshot Serengeti	B03
C28	NZ Trail Cam. Animals	EFH_HCAME02	C86	NA Camera Trap Img	lebec_CA-20
C29	NZ Trail Cam. Animals	EFH_HCAMA02	C87	Snapshot Serengeti	G07
C30	Snapshot Serengeti	U12	C88	Snapshot Serengeti	O09
C31	NZ Trail Cam. Animals	PS1_CAM7709	C89	Snapshot Serengeti	I12
C32	NZ Trail Cam. Animals	EFH_HCAMA09	C90	Wellington Camera Traps	031c
C33	NZ Trail Cam. Animals	EFH_HCAME01	C91	Snapshot APNR	K051
C34	NZ Trail Cam. Animals	EFD_DCAME02	C92	Caltech Camera Trap	46
C35	Snapshot Madikwe	G08	C93	Snapshot Madikwe	B03
C36	NZ Trail Cam. Animals	EFH_HCAMA05	C94	NZ Trail Cam. Animals	EFH_HCAME05
C37	Snapshot Camdeboo	E02	C95	Snapshot Karoo	A01
C38	Orinoquía Camera Traps	N07	C96	Snapshot Madikwe	D07
C39	NZ Trail Cam. Animals	EFD_DCAMB02	C97	Idaho Camera Traps	122
C40	NZ Trail Cam. Animals	EFD_DCAME07	C98	Snapshot Serengeti	L07
C41	NZ Trail Cam. Animals	EFD_DCAME01	C99	Snapshot Serengeti	O13
C42	Orinoquía Camera Traps	M00	C100	Snapshot Madikwe	A04
C43	Snapshot Serengeti	G13	C101	NA Camera Trap Img	lebec_CA-21
C44	NA Camera Trap Img	lebec_CA-16	C102	NA Camera Trap Img	lebec_CA-36
C45	NZ Trail Cam. Animals	EFH_HCAMB09	C103	Snapshot Paarl Mtn.	B04
C46	Snapshot Camdeboo	B04	C104	Snapshot Serengeti	O10
C47	NZ Trail Cam. Animals	EFD_DCAMA02	C105	Snapshot Serengeti	Q11
C48	Snapshot Serengeti	E01	C106	Snapshot APNR	U43B
C49	Snapshot Serengeti	E13	C107	Caltech Camera Trap	100
C50	NZ Trail Cam. Animals	EFH_HCAME06	C108	Idaho Camera Traps	85
C51	Snapshot Kgalagadi	KHOLA08	C109	Snapshot Mt. Zebra	F04
C52	Orinoquía Camera Traps	N04	C110	Snapshot Ruaha	M7
C53	NZ Trail Cam. Animals	EFH_HCAME03	C111	Snapshot APNR	K023
C54	NZ Trail Cam. Animals	EFH_HCAME12	C112	Caltech Camera Trap	70
C55	NZ Trail Cam. Animals	EFH_HCAMA06	C113	Snapshot Enonkishu	B02
C56	NZ Trail Cam. Animals	EFD_DCAMA08	C114	NZ Trail Cam. Animals	EFD_DCAME07
C57	NZ Trail Cam. Animals	EFH_HCAME04	C115	Snapshot APNR	N1
C58	NZ Trail Cam. Animals	EFH_HCAME04	C116	NZ Trail Cam. Animals	EFD_DCAME03